PRE-PRECIPITATION AND PRECIPITATION IN ALUMINIUM MANGANESE ALLOYS

A Thesis Submitted
In Partial Fulfilment of the Requirements
for the Degree of
MASTER OF TECHNOLOGY

By
VIJENDRA SINGH

to the

DEPARTMENT OF METALLURGICAL ENGINEERING
INDIAN INSTITUTE OF TECHNOLOGY KANPUR
JULY 1975

CERTIFICATE

This is to certify that the work PRE-PRECIPITATION AND PRECIPITATION IN ALUMINIUM-MANGANESE ALLOYS' has been carried out by Mr. Vijendra Singh under my supervision and that it has not been submitted else-where for a degree.

T.R.Ramachandran

(T.R. Ramachandran)
Assistant Professor
Department of Metallurgical Engineering
Indian Institute of Technology
Kanpur, India.

ACKNOWLEDGEMENTS

The author wishes to acknowledge gratefully the encouragement and aid extended by Dr. T.R. Ramachandran. He thanks Dr. A.K. Jena for allowing to use the laboratory facilities and for very useful discussions.

The author acknowledges the assistance of Mr. Jogender Singh, without whose help the work would have been difficult, Mr. Nirbhay Singh, Mr. S.Kumar, Mr. B.P. Kashyap for constant encouragement and help.

The author acknowledges the assistance of :
Mr. K.P. Mukherjee for various sundry help, and Mr. G.L. Misra for typing the manuscript.

Dr. S.K. Sachdeva, Principal, Panjab Engineering College is thanked for granting the author leave of absence for a period of two years to complete this work.

Last but not the least, he admires the patience shown by his wife Manjari, and son, Samerendra during this period.

TABLE OF CONTENTS

LIST OF TABLES

LIST OF FIGURES

SYNOPSIS

Pre-precipitation and precipitation in Al-Mn alloys

The binding energy of the manganese-vacancy complex (B_{V-Mn}) in an aluminium - ~0.35 wt.% manganese alloy is determined by carrying out electrical resistivity measurements on the quenched alloy. Two different techniques are used for the evaluation of B_{V-Mn} - one based on the temperature dependence of the as-quenched resistivity (thermodynamic method) and the other on the rate of decay of quenched-in vacancies (Kinetic method). The thermodynamic method yields a value for B_{V-Mn} of 0.21 eV. The Kinetics of annealing of vacancies in pure Al in the temperature range 0 - 30°C follow the first order Kinetics giving a value of 0.65 eV for the migration of single vacancy in pure aluminium. The rate of decay of excess vacancies in the aluminium - manganese alloy does not obey the first order kinetics. On the basis of a model involving simuntaneous annealing of single- and di-vacancies B_{V-Mn} is estimated to be 0.1 eV. An analysis of the errors involved in the two techniques indicates that the value of 0.1 eV is more reliable. Preliminary work on the isothermal annealing of quenched Al- 1.0 wt % Mn alloy shows that the precipitation is sluggish even at temperatures of the order of 500°C.

CHAPTER 1

INTRODUCTION

"Vacant sites and interstitial atoms are generated in significant numbers by thermal fluctuation and possess an equilibrium density dependent on temperature -

J. Frenkel."

All real crystals contain a variety of imperfections. These imperfections can be, broadly, divided into two classes - point defects and extended defects. As the name implies, point defects are highly localised and are characterized by disturbance around a single atomic site. As is well known, a perfect crystal is thermodynamically stable only at absolute zero, and at any higher temperature, the crystal must contain a certain number of point defects. The elementary point defects in a pure metal are vacancies and interstitials. Vacancy is a missing atom in the periodic array of atoms, while interstitial is an atom located in a non-lattice position in the array. Point defects are the only type of defects which can exist in thermal equilibrium in the materials. Point defects can interact with each other. The interaction of a vacancy and an interstitial leads to the interstitial occupying a normal lattice site with the annihilation of both the defects. Vacancies can cluster to form a divacancy, a trivacancy etc., leading even to the formation of a void or a dislocation loop, under certain conditions.

The extended defects are disturbances in the regular array of atoms which extend over many lattice distances. Such defects are accidents of growth and are not in thermodynamic equilibrium. The extended defects include the dislocations, surfaces, grain boundaries, stacking faults, etc. Point defects can also interact with extended defects. It is well known that extended defect act as sources and sinks for vacancies.

The high energy requirements for the formation of an interstitial atom as illustrated by the theoretical calculations[1] resulted in the conclusion that in F.C.C. metals, interstitial atoms constitute a negligible fraction of the equilibrium vacancy concentration at any given temperature.

Johnson[2] predicted the interaction of vacancies with solute atoms forming solute-vacancy complexes. The concentration of the latter depends on the magnitude of the solute-vacancy binding energy, B_{Vi}, which is defined as the difference between the energies required for a vacancy to form in the solute-free lattice, and in a site adjacent to a solute atom. When B_{Vi} is positive, the equilibrium concentration of vacancies in a pure solvent is less than that in its alloy at a constant temperature[3]. This difference is a function of B_{Vi}, concentration of solute and temperature.

Experimental studies on the formation and migration energies of vacancies in metals and alloys have assumed considerable importance

in the recent years. A study of the temperature dependence of the concentration of vacancies in metals and alloys (Thermodynamics method) enables the estimation of the formation energy of a vacancy in a pure metal and the solute-vacancy binding energy in the alloy. The migration energy of the vacancy can be determined by studying the rate of decay of an excess concentration of vacancies (Kinetic method) in a metal or alloy. The sum of the formation and migration energies must be equal to the activation energy for diffusion if vacancy mechanism is operative in the diffusion process.

The process of solute clustering in many alloys, when they are quenched from high temperature and subsequently aged, is associated with the presence of vacancies in supersaturated condition in the quenched alloys[4,5]. As the clustering process is related to the age-hardening phenomenon in alloys, the presence of excess vacancies will have a profound effect on the age-hardening process. For example, age hardening is reported to be retarded by the presence of In, Cd, and Sn as impurities in Al-Cu alloy as these elements, having high solute-vacancy binding energy compared to Cu allow only a small number vacancies for the solute transport operation necessary for the clustering process[6]. Quenched in vacancies also affect the process of precipitation from supersaturated solid solution for example, the precipitation of silicon from supersaturated solid solution[7,8] is accelerated by excess vacancies.

Transition metals are commonly used as addition elements to aluminium alloys. Although they do not produce age hardening or large solution hardening properties they are useful in inhibiting recrystallisation, preventing stress corrosion and improving weldability. The commercial aluminium alloy, AA 3003, contains about 1.0 to 1.5 wt. % Mn and is normally employed in the work hardened condition. The formation of a number of metastable phases in the aging of supersaturated Al-Mn alloys is well documented[8]. However there is hardly any work reported on the kinetics of precipitation in the aluminium - manganese alloys.

The binding energy of the manganese - vacancy complex has been determined by two different techniques[6,9,10]. The thermodynamic method as discussed in chapter 2 involves the rapid quenching of vacancies in thermal equilibrium at high temperatures to low temperatures and measuring the concentrations of the frozen-in vacancies. These excess vacancies tend to anneal out at temperatures where the vacancies are mobile. The rate of annealing in alloys is related to the binding energy of the solute-vacancy complex and the migration energy of the vacancy in pure metal. This forms the basis for the kinetic method of estimating solute-vacancy binding energy. Quantitative treatments for these methods are given in the next chapter. While several techniques can be used for the measurement of the vacancy concentrations, the most reliable and widely used one is electrical resistivity measurements. This technique is of immense use in studying the excess concentration of vacancies present at any temperature. In this

investigation the binding energy of the manganese - vacancy complex is computed by electrical resistivity measurements of excess vacancies in an aluminium - 0.35% manganese alloy. This work is a follow up of the investigations in an aluminium - 0.1 wt. % managanese alloys carried out in our laboratory[11].

CHAPTER 2

REVIEW OF PREVIOUS WORK

This chapter deals with the thermodynamics of point defects and the kinetics of their annealing out along with a review of the work already done.

2.1 THERMODYNAMICS OF VACANCIES IN METALS

Generation of vacancies in a crystal increases its internal energy, since it requires a certain amount of positive work. As there are many ways of distributing the point defects on the available lattice sites, the configurational or mixing entropy is also increased. So, the balance between energy and entropy terms will lead to a minimum in the free energy for a certain concentration of vacancies at any temperature, T, above the absolute zero. The number of ways, W in which n vacancies can be arranged on N lattice sites is

$$W = \frac{N(N-1)\ (N-2)\ \text{---}\ (N-n+2)(N-n+1)}{n!} \qquad (2.1)$$

$$= \frac{N!}{(N-n)!\ n!} \qquad (2.2)$$

The configurational entropy, S, is given from statistical mechanics as

$$S = k \ln W = k \ln \frac{N!}{(N-n)!n!} \qquad (2.3)$$

where k is the Boltzmann constant. Using Stirling's approximation, viz.

$\ln x! = x \ln x - x$, for $x >> 1$, we get

$$S = k [N \ln N - (N-n) \ln (N-n) - n \ln n] \tag{2.4}$$

If E_V^f is the energy to form one vacancy, then the increase in free energy, ΔF, of a crystal containing n vacancies at T°K is given by

$$\Delta F = n E_V^f - TS \tag{2.5}$$

$$= n E_V^f - kT [N \ln N - (N-n) \ln (N-n) - n \ln n] \tag{2.6}$$

At equilibrium,

$$\left(\frac{\partial \Delta F}{\partial n}\right) = 0 = E_V^f - k T \ln \left(\frac{N-n}{n}\right)$$

thus $$\frac{n}{(N-n)} = e^{-E_V^f/kT} \tag{2.7}$$

As $n << N$, the atomic fraction (C_V) of monovacancies is given by

$$C_V = \frac{n}{N} = e^{-E_V^f/kT} \tag{2.8}$$

The equation (2.8) reveals that vacancy concentration is zero at absolute zero and increases exponentially as the temperature is raised. So far, we have neglected all the entropy changes other than configurational entropy. The equation (2.8) can be written in general, as,

$$C_V = \exp (S_V^f/k). \exp (-E_V^f/kT) = A \exp (-E_V^f/kT) \tag{2.9}$$

where S_V^f is the entropy of formation. A is normally assumed to be unity.

By similar thermodynamic calculations, the concentration of di-vacancies, C_{2V} in a metal at temperature T can be shown to be

$$C_{2V} = \frac{n_2}{N} = \frac{1}{2} Z (C_V)^2 e^{B_2/kT} \qquad (2.10)$$

where, Z is the coordination number of lattice, B_2 is the binding energy of a di-vacancy which is defined as $2E_V^f - E_{2V}^f$, where E_{2V}^f is the energy of formation of a divacancy.

2.2 THERMODYNAMICS OF VACANCIES IN DILUTE BINARY ALLOYS :

In binary alloys, apart from the above considerations, a solute atom and a vacancy, next to the solute atom, can interact. When this interaction energy or solute-vacancy binding energy B_{Vi} is positive, it is energetically favourable for the vacancies to form next to the solute atoms, a tendency opposed by entropy considerations.

The total vacancy concentration, C_V^I , in an alloy is the sum of the free vacancy concentration, C_V, and the bound vacancy concentration C_{Vi}. Following Loner[3], these are given by,

$$C_V = A (1 - \overline{Z+1}\ I_o) \exp (-E_V^f/kT) \qquad (2.11)$$

and $$C_{Vi} = A Z I_o \exp [-(E_V^f - B_{Vi})/kT] \qquad (2.12)$$

where A is the entropy factor, assumed to be the same for free and bound sites, E_V^f is the energy of formation of a vacancy in a pure solvent, I_o is the solute concentration.

$$\text{So, } C_V^1 = A \exp(-E_V^f/kT)\left[1 - \overline{Z+1}\, I_o + Z\, I_o \exp(B_{Vi}/kT)\right]$$

$$= C_V\left[1 - \overline{Z+1}\; I_o + Z\, I_o \exp\left(\frac{B_{Vi}}{kT}\right)\right] \qquad (2.13)$$

which means that the total vacancy concentration in an alloy is greater than that in pure metal by an amount which depends on B_{Vi}, I_o and T. The vacancies in an alloy are partitioned between bound and unbound (free) sites. The proportion of the former increases with increase in B_{Vi} and decrease in temperature.

The binding energy of a solute to a vacancy is due to a strain energy term, ΔB_S and an electrostatic interaction term, ΔB_C. The strain in the lattice, caused by the presence of large sized solute, can be relieved by the presence of a vacancy adjacent to it. For solutes in noble metal matrix, ΔB_S is expected to have values between 0.03 to 0.27 eV based on size effect[12]. The presence of a hetero-valent solute atom in a solvent, causes the latter to be repelled by a coulomb force in addition to the normal closed-shell repulsion, which reduces the binding energy of these atoms. For noble metals, ΔB_C is positive for solutes of higher valency, being 0.1 eV for quadrivalent solute and 0.12 eV for pentavalent solute[12].

2.2.1 Nucleation of Vacancies

We know that there is an exponential increase in the concentration of vacancies with increase in temperature. Let us see how such large concentrations are generated. The idea of nucleating

all of them by Frankel pairs is rejected on the basis that high energies are required for nucleating these pairs ($\sim$ 3 eV). The main source for generating vacancies must be in extended defects like dislocations, grain boundaries, free surfaces etc, where there is no need to form an interstitial for every vacancy generated. When free surfaces are made of high index planes, the kink sites can act as sources of vacancies. This process can continue until surface assumes low-index orientation. Dislocations play a very important role in generating vacancies. The pulse-heating experiment of Jackson[13], Koehler and Lund[14] indicate the attainment of a uniform vacancy concentration in a grain by heating it for a few milli seconds. This uniform concentration cannot be attained, as shown by theoretical diffusion calculations, by diffusion from the surfaces and grain boundaries alone, indicating the important role of dislocations in vacancy generation. The climb of edge dislocations results in the generation or absorption of point defects under conditions of under or super-saturation. Vacancies can also be nucleated from high angle boundaries.

2.3 QUENCHED-IN VACANCIES IN METALS :

The sample soaked at a high temperature, T_q, is cooled rapidly (β is the rate of quenching) to a lower temperature, T_b, to retain a high concentration of vacancies. So, T_q, T_b and β play very important role in controlling the concentration of excess vacancies produced. T_q must be high enough to have large concentrations of

defects for precise measurement. But the clustering of defects increases with the rise in quench temperature and also aggregation of defects takes place during the quenching itself. If single defects are of interest, the clustering process puts an upper limit to the quench temperature but the requirement of a measurable amount sets a lower limit for the quenching temperature.

Depending on the binding energy, the concentration of the clusters of vacancies increases during quenching at the expense of single vacancies. When single and divacancies alone are considered, there is a critical temperature, T*, below which the equilibirum between C_V and C_{2V} is frozen. For Aluminium, this temperature is given by the equation[15]

$$\frac{7k\,\nu_3}{B_2\,\beta} = \frac{\exp\ (E_m + B_2)/kT^*}{[1+48\ C_V \exp B_2/kT^*]^{1/2}} \qquad (2.14)$$

where ν_3 is vibrational frequency of atoms which are the nearest neighbours of a vacancy and E_m is the single vacancy migration energy. It is found that the number of di-vacancies formed during the quench increases with an increase in quenching temperature, di-vacancy binding energy and with decreasing quenching rate[16].

T_b must be sufficiently low to prevent the loss of retained vacancies before and during the measurements. Normally the samples are quenched in ice or brine and transferred to liquid Nitrogen. The measurement are made at the liquid N_2 Temperature. The cooling rate

β must be high enough to retain a major portion of vacancies. The high cooling rates will cool the outer layer of sample rapidly, which will contract. This process will cause the plastic deformation of relatively warm core. Jackson[17] has shown that plastic deformation causes increased vacancy sink concentration rather than the production of vacancies. This effect on concentration of vacancies and also on kinetics of annealing, limits the quenching rate to produce no plastic deformation.

2.4 ELECTRICAL RESISTIVITY OF QUENCHED-IN VACANCIES

The electrical resistivity of materialsis increased by the introduction of defects into the lattice[18]. The presence of imperfections causing a disturbance of the ideally periodic lattice results in the scattering of the conduction electrons and hence an increase in the electrical resistance, the magnitude of which is proportional to the concentration of defects. When a metal is at a high temperature, it has defects in thermal equilibrium. The quenching of this metal to a lower temperature leads to freezing of these defects. These defects, in excess of those in thermal equilibrium pertaining to the lower temperature, give rise to an extra-resistivity to the metal. In a pure metal, the extra-resistivity, $\Delta\rho$, due to quenching, is related to the concentration of vacancies by the equation,

$$\Delta\rho = A \times \rho_V \exp\left(-F_V^f / k\, T_q\right) \qquad (2.15)$$

where x is the fraction of the vacancy concentration in equilibrium at the quenching temperature, T_q, retained by the quench and ρ_V is the resistivity per unit fractional vacancy concentration. A plot of ln $\Delta\rho$ against $1/T_q$ is therefore linear, with the slope equal to $-E_V^f/k$ and intercept equal to $Ax\ \rho_V$.

In interpreting the quenched-in resistivity of dilute alloys, allowance be made for the fact that resistivity of unit fractional concentration of bound vacancy, ρ_{aV}, is different from that of a free vacancy, ρ_V. The extra resistivity, $\Delta\rho_a$, in a quenched f.c.c. alloy is given by[19]

$$\Delta\rho_a = Ax' \rho_V \exp(-E_V^f/k\ T_q)\ [1-13\ I_o + 12\ I_o\theta\ \exp B_{Vi}/k\ T_q] \quad (2.16)$$

where x' is the appropriate value of x for the alloy and $\theta = \rho_{aV}/\rho_V$.

$$\therefore \frac{\partial(\ln \Delta\rho_a)}{\partial(1/T_q)} = \frac{1}{k}\left[E_V^f - \frac{12\theta\ I_o\ B_{Vi}\ \exp(B_{Vi}/k\ T_q)}{1-13\ I_o + 12\ I_o\ \theta \exp(B_{Vi}/k\ T_q)}\right] \quad (2.17)$$

It is found experimentally that if $\Delta\rho_a$ is measured for different quench temperatures over a narrow range, a plot of ln $\Delta\rho_a$ against $1/T_q$ is a straight line with the slope defining an apparent activation energy E_V^{f*},

$$\frac{\partial(\ln \Delta\rho_a)}{\partial(1/T_q)} = -\frac{E_V^{f*}}{k} \quad (2.18)$$

Comparing two equations (2.17) and (2.18), we get

$$E_V^f - E_V^{*f} = \Delta E = \frac{12\,\theta\, I_o\, B_{Vi} \exp\,(B_{Vi}/k\,T_q)}{1-13\,I_o + 12\,I_o\,\theta \exp\,(B_{Vi}/k\,T_q)} \qquad (2.19)$$

For using equation (2.19), the relationship between ΔE and B_{Vi} is computed for various values of I_o, θ, and T_q and the computed curves are used to derive B_{Vi} from the experimentally measured values of $(E_V^f - E_V^{*f})$. This method is termed thermodynamic method as the basic equations (2.15) and (2.16) are similar to thermodynamic equations (2.9) and (2.13).

2.5 KINETICS OF ANNEALING OF QUENCHED-IN VACANCIES :

As already shown, vacancies can be retained in a metal in excess of the thermodynamic equilibrium concentration. This thermodynamic driving force reduces the concentration of these vacancies to the equilibrium concentration, characteristic of the temperature. Annealing is the process of disappearance of the super-saturation of defects. Since the mobility of defects increases rapidly with increasing temperature, a suitable temperature interval can always be found in which the rate of disappearance of a given defect can be measured. The annealing may occur as a single or a multi-step process. The isochronal annealing of a quenched sample involves heating it to successively higher temperatures with the time of heating at each temperature being fixed. The attendant changes in vacancy concentration (measured by the changes in electrical resistivity) at the end of each heating step can establish the annealing stages. Once the annealing

stages are identified, the kinetics of each stage may be studied to determine the activation energies associated with the processes.

2.5.1 Isothermal Annealing

Federighi et al[20,21] performed isochronal annealing of quenched 99.995% pure Al for a period of 2 minutes at each temperature. The results are shown in Figure 1. There are two isochronal stages. They observed that the largest fraction of the quenched-in resistivity anneals out in stage I occuring at or below room temperature. This stage I is due to the formation of dislocation loops and voids by vacancy condensation as shown by transmission electron microscopy[22,23] Federighi et al also observed similar results for dilute Al alloys.

The simplest annealing process is that in which single vacancies diffuse to a fixed number of unfillable sinks. The long time solution for the process indicates a simple exponential decay of vacancies. The number, n, of defects remaining in the metal changes according to the relation,

$$\frac{dn}{dt} = - Kn \qquad (2.20)$$

where K is a rate constant independent of n and proportional to the diffusion coefficient, D, for the annealing species. So,

$$n = n_o e^{-Kt} \qquad (2.21)$$

where $K = \alpha D$, where α is identified with sink concentration.

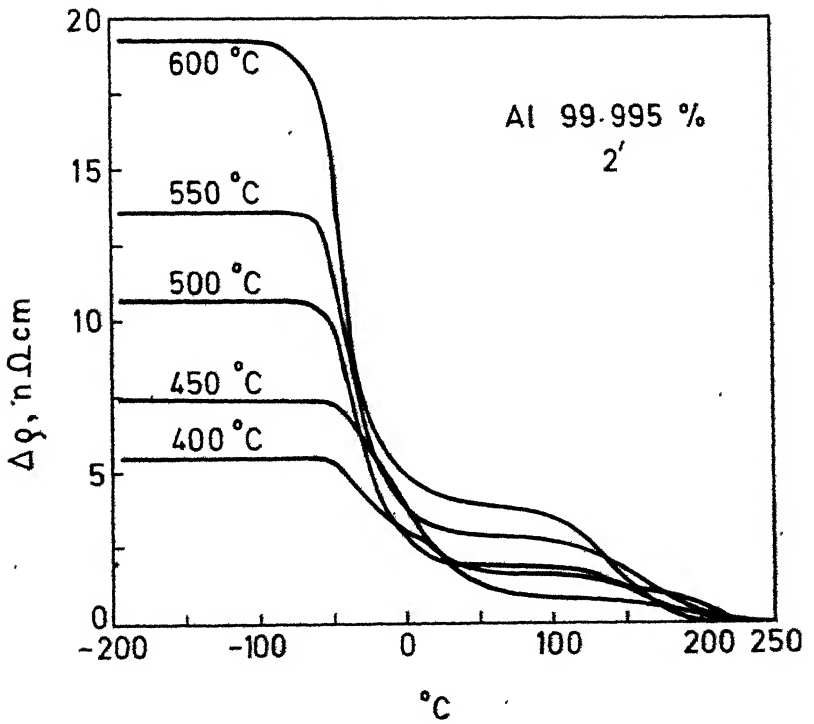

FIG.1. Isòchronal annealing of pure Al.

In dilute alloys, every vacancy encounters a large number of solute atoms during its diffusion to sink. If the vacancy-solute complex is immobile or has lower mobility than that of free vacancy, the vacancy is trapped and the complex must dissociate before the vacancy can migrate to a sink.

Damask and Dienes[1] gave the following theoretical treatment symbolising the annealing process by two chemical equations. They had assumed that the defect concentration is low enough to neglect the interaction of vacancies with one other and with vacancy-impurity complexes, and the diffusion of vacancy to sinks is described by a first order process.

$$V + I \underset{K_2}{\overset{K_1}{\rightleftharpoons}} C \qquad (2.22)$$

$$V \xrightarrow{K_3} \text{sinks} \qquad (2.23)$$

where V, I, and C are the concentrations (atomic fractions) of vacancies, unbound impurity atoms, and vacancy - impurity complexes, respectively, and the K's are the corresponding rate constants. The differential equations for these reactions can be written (after the substitution $I = I_o - C$) as

$$\frac{dc}{dt} = K_1 I_o V - K_1 C V - K_2 C \qquad (2.24)$$

$$\frac{dV}{dt} = -K_1 I_o V + K_1 C V + K_2 C - K_3 V \qquad (2.25)$$

where I_o is the total impurity concentration. The total vacancy concentration is described by the differential equation

$$\frac{dN}{dt} = \frac{d(C+V)}{dt} = \frac{dC}{dt} + \frac{dV}{dt} = -K_3 V \qquad (2.26)$$

Equations (2.24) and (2.25) form a set of nonlinear coupled differential equations which, when solved, will describe the complete annealing behaviour of the system. The equlibrium vacancy concentration at the annealing temperature is negligible, and so, V and C approach zero as time approaches infinity. Analog computer solution (for a variety of parameters) of these equations showed that the number of complexes, C, increased very rapidly during the early stages of annealing, and during this transient period, the free vacancy concentration decreased rapidly. After these transients, C and V decayed steadily. The transients correspond the establishment of equilibrium between V and C, characteristic of the annealing temperature. The rapid elimination of these transient conditions suggests that an analytic approximation could be used for the bulk of the vacancy decay curve. Equilibrium for the reaction given by equation (2.22) implies that

$$\frac{C}{V(I_o - C)} = \frac{K_1}{K_2} \qquad (2.27)$$

which, incidentally, is also the condition for the steady-state approximation on C, i.e., $\frac{dC}{dt} = 0$. Many of the decay curves were found to be simple exponential in time i.e. $\frac{C}{V}$ remains constant. This is obtained when a further approximation namely $C << I_o$, is made, we get

$$\frac{C}{V} = I_o \frac{K_1}{K_2} \qquad (2.28)$$

Substitution of equation (2.28) in (2.26) and integration gives,

$$C + V = N = V_o' \left[1 + (I_o K_1/K_2 \right] \exp -(-K_e t) \qquad (2.29)$$

where V_o' is the free vacancy concentration at the beginning of the exponential decay and,

$$K_e = \frac{K_3}{\left[1 + I_o \frac{K_1}{K_2}\right]} \qquad (2.30)$$

The various rate constants are given by

$$K_1 = 84\ \nu \exp\ (-E_m/kT) \qquad (2.31)$$

$$K_2 = 7\ \nu \exp\ [-\ (E_m + B_{Vi})/kT] \qquad (2.32)$$

$$K_3 = \alpha\ \nu\ \lambda^2 \exp\ [-\ E_m/kT\ ] \qquad (2.33)$$

where 84 and 7 are the appropriate combinatory numbers for association and dissociation of complexes in F.C.C. lattice, α is the vacancy sink concentration, ν is the jump frequency and λ is the jump distance. Therefore, for solute-vacancy interaction

$$\frac{K_1}{K_2} = 12 \exp\ \left(\frac{B_{Vi}}{kT}\right) \qquad (2.34)$$

The equation (2.30) can now be rewritten as ,

$$K_e = \frac{K_3}{1 + 12\ I_o \exp\ \left(\frac{B_{Vi}}{kT}\right)} \qquad (2.35)$$

As K_3 can be determined by annealing experiment on a pure sample and K_e can be found out by similar experiment on an alloy at the same temperature, B_{Vi} can be found out by equation (2.35).

When the quenching temperatures are high divacancies will be formed. There will be a simultaneous annealing out of single and di-vacancies to fixed sinks, the kinetic equations can be written now,

$$V + I \underset{K_2}{\overset{K_1}{\rightleftharpoons}} C$$

$$V + V \underset{K_5}{\overset{K_4}{\rightleftharpoons}} V_2$$

$$V \xrightarrow{K_3} \text{sinks}$$

$$V_2 \xrightarrow{K_6} \text{sinks} \ .$$

The differential equation can be written similarly after substitution $I = I_o - C$ as

$$\frac{dV}{dt} = - K_1 V I_o + K_1 V C + K_2 C - K_4 V^2 + K_5 V_2 - K_3 V \qquad (2.36)$$

$$\frac{dV_2}{dt} = \frac{1}{2} K_4 V^2 - \frac{1}{2} K_5 V_2 - K_6 V_2 \qquad (2.37)$$

$$\frac{dC}{dt} = K_1 V I_o - K_1 V C - K_2 C \qquad (2.38)$$

As the total vacancy concentration $N = V + 2 V_2 + C$

$$\text{So, } \frac{dN}{dt} = \frac{dV}{dt} + 2 \frac{dV_2}{dt} + \frac{dC}{dt} = - K_3 V - 2K_6 V_2 \qquad (2.39)$$

The rate constants K_4, K_5 and K_6 are given by

$$K_4 = 84 \nu \exp (- E_m/kT)$$

$$K_5 = 14 \nu \exp [-(E_m + B_2)/kT]$$

$$K_6 = \alpha \nu \lambda^2 \exp\left[-\frac{E_{m(2)}}{kT}\right]$$

where $E_{m(2)}$ is the migration energy of divacancy.

Chik[24] has solved equation (2.39) with a steady state approximation on di-vacancies i.e., $\frac{dV_2}{dt} = 0$. For weak solute-vacancy binding energy, his solution is

$$\frac{1}{V} = \left[\frac{1}{V_o'} + \beta\right] \exp\left[\frac{K_3 t}{1 + \frac{K_1}{K_2} I_o}\right] \qquad (2.40)$$

where $\beta = \frac{2K_4 K_6}{K_3(K_5+K_6)}$.

For this solution, it has been assumed that solute-vacancy complex is immobile and the formation of divacancy - impurity complex is neglected. The Computer solution[11] of differential equations (2.36) to (2.39) indicates that the steady state approximation is incorrect.

2.6 ISOTHERMAL ANNEALING AT HIGH TEMPERATURES

The high temperature decomposition of Al-Mn (1-10 wt % Mn) alloy should lead to precipitation of the equilibrium Al_6 Mn phase. Other metastable precipitates also appeared in the structures, dependent whether the isothermal annealing temperature was above or below 550°C. Nes et al[8] examined Al - 1.8 wt % Mn alloy at 460°C. The short time annealing gave three different products, of which one was metastable cubic G phase with b.c.c. structure ($a = 7.54 \pm 0.08$ A°) and the other two phases, denoted G' and G'' were simple cubic

($a = 12.75 \pm 0.15$ A°) and hexagonal ($a = 7.54 \pm 0.07$, $C = 7.84 \pm .08$ A°) respectively. The relative amount of G phase increased with increasing annealing time. G phase nucleated preferentially on both G' and G'' particles. G'' phase has been suggested as a metastable phase in this whereas G' as impurity induced phase.

Little et al[33] had observed that "G'' phase got dissolved when isothermal annealing at 600°C was done for 24 days, and it dissolved in much lesser amount when isothermally annealed at 550°C for 40 days but its proportion remained nearly constant when isothermally annealed at 460°C for 40 days.

The kinetics of precipitation in Al-Mn (1 wt %) alloy have been incompletely studied by Lahiri[11] in range 425° to 550°C for very short times. Studies have been made, in this investigation, on this alloy for isothermal annealing in the range 400° to 550°C for much longer times such as 42 days.

CHAPTER 3

EXPERIMENTAL PROCEDURE

3.1 MATERIALS STUDIES :

The present investigation necessitated the use of the following materials :

i) Pure aluminium, 99.999% pure

ii) Aluminium - 0.35 wt % manganese alloy

iii) Aluminium - 1.00 wt % manganese alloy

The alloys were prepared from 99.999% pure Al and 99.999 % pure Mn.

3.2 PREPARATION AND PROCESSING OF ALLOYS

The required weighed quantities of pure metals, after cleaning with hydrochloric acid were melted in high purity alumina crucible putting it in an electric muffle furnace. The ingots after homogenising at 625°C for 72 hours were hot forged to a size of 12.5 mm. diameter rods which were swagged in stages with intermittent annealing to a size of 2.5 mm diameter rods. They were cold rolled with intermittent annealing to size of 0.85 mm x 0.85 mm. The present investigation had been carried out on the wires prepared by Lahiri[11]. The results of spectroscopic analysis of alloys are given in Table 1.

Table 1

Results of Spectroscopic Analysis of used alloys :

Alloy	wt % Mn	Elements present in trace (< 0.001 wt %)	Elements not detected
Al-0.35 wt% Mn	0.35	Cu	Zn, Si, Fe, Cr, Mg Ni, Ti
Al-1.00 wt % Mn	1.00	Mg Cu	Si, Fe, Ni, Cr, Cd.

3.3 SAMPLE PREPARATION

A wire of pure Al or alloy of about 70 cms, after cleaning, was wound to a helical coil of about 7 mm internal diameter with about 3 cms of straight lengths at each end. As the measurement of low resistance necessitates the use of separate current and potential leads at each end of sample, four wires of about 70 cms length were taken fusing two of them to each end of the sample. The following flux was used for fusion :

Sodium chloride 32% by wt ; Sodium flouride 15% by wt,

Lithium chloride 27% by wt, Potassium chloride 26% by wt.

The details of joining the leads are described in the work of Lahiri[11].

A slight modification had been made to the sample assembly used by Lahiri[11] as shown in Figure 2. All the four leads were insulated with refractory beads to a length of about 45 cms. from the junction of the lead wires and the specimen. To facilitate identification of lead wires coming from one end of the sample, one

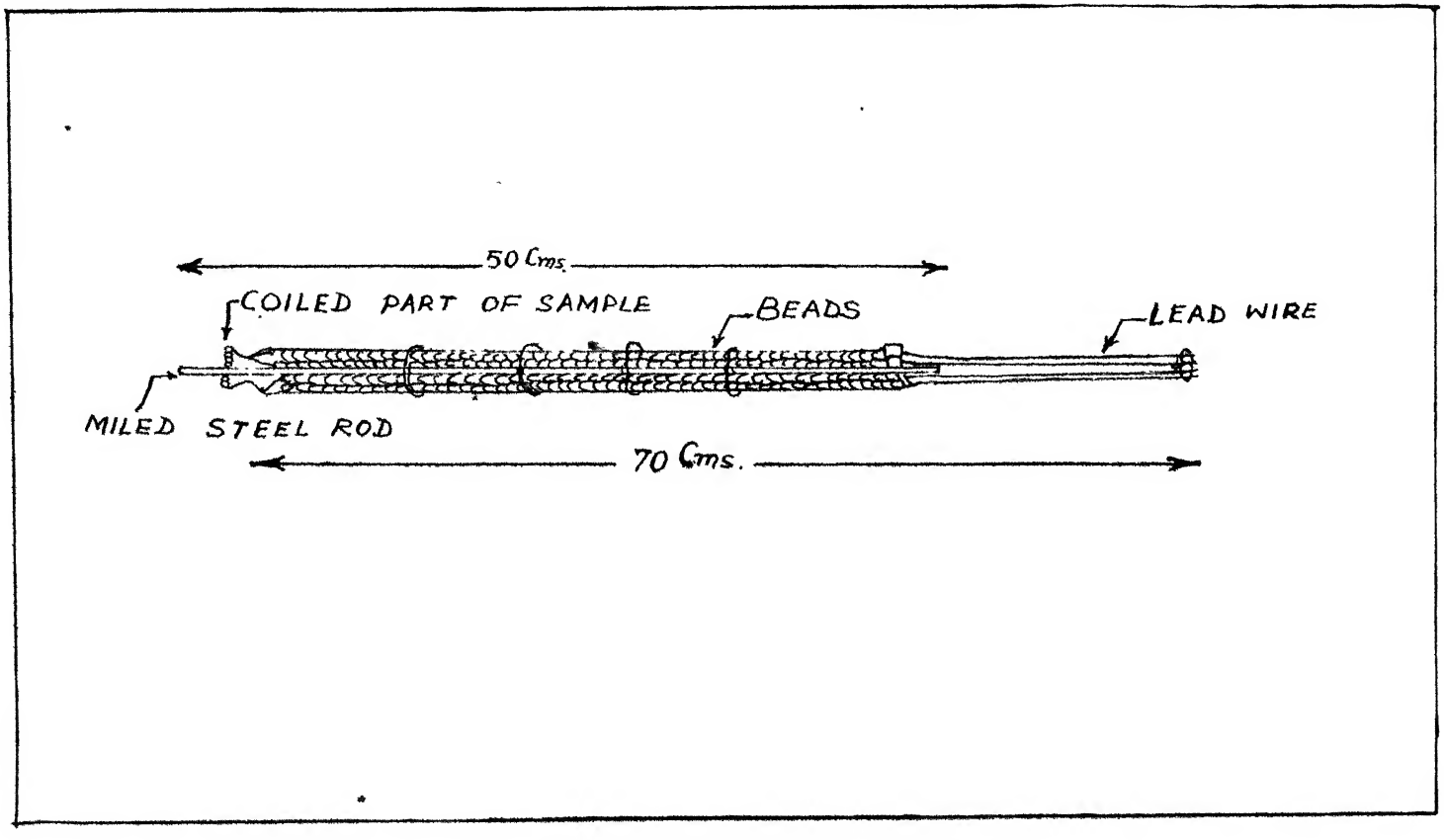

FIG. 2 SAMPLE ASSEMBLY

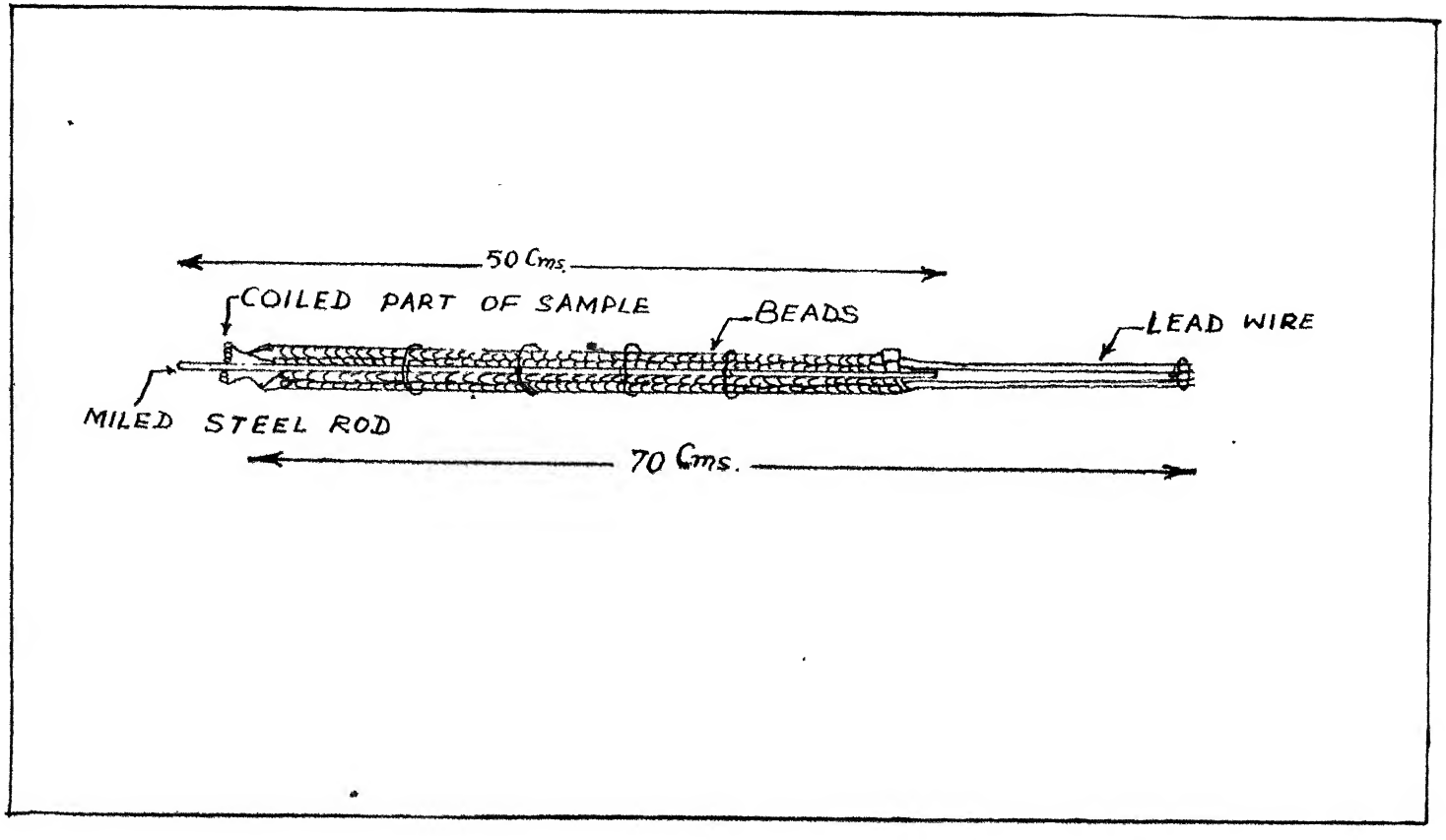

FIG. 2 SAMPLE ASSEMBLY

large sized bead was put, at the end, in each of the two wires coming from one end of the specimen. One mild steel rod of 50 cms. length and 2.5 mm dia. was taken and four grooves at a distance of 12 cms. from one end and from each other were made on it. The sample assembly was tied to this mild steel rod by pure Al wire making sure that the Al wire was not touching the lead wires. The grooves, in mild steel rod, helped in keeping the specimen tightly attached to the rod. The four ends of lead wires were tightened. This arrangement allowed the quick fall of the sample during quenching. While measuring the resistance of the sample, the possible short circuiting of the lead wires was prevented by inserting them into 4 holes made on a neoprene sheet. The portion of the lead wires, above the neoprene sheet, was bent through 90° to facilitate easy handling of the sample. The neoprene sheet was taken out, and the lead wires held in position by Al wire, whenever high temperature heating was done.

3.4 ELECTRICAL RESISTANCE MEASUREMENT SET UP :

The following well known relationship gives the electrical resistivity of the sample

$$\rho = \frac{R}{(\ell/A)} \qquad (3.1)$$

where R is the resistance of the sample in Ohms, ℓ is the length of sample in cms, A is the cross-sectional area of the sample in cm^2 and ρ is the resistivity of the material in Ohm-cm. As the

present investigation requires the measurement change in resistivity, the equation (3.1) is written as

$$\Delta\rho = \frac{\Delta R}{(\ell/A)} \qquad (3.2)$$

we see from equation (3.2) that the variation in resistivity, $\Delta\rho$, will be directly proportional to the variation in resistance, ΔR, since the ℓ/A ratio for a particular sample remains constant. The length and area were chosen as a compromise for precise measurement of resistivity and the maximum resistance that can be measured on the Kelvin Bridge. Table 2 shows the (ℓ/a) ratio used for some samples.

For accurate measurement of resistance of the sample, Kelvin bridge had been used. The circuit diagram of it is shown in Figure 3, where X is the resistance to be measured, R is the movable resistance for comparison, A and B are calibrated resistance in main ratio arms of the circuit and a and b are the calibrated resistances in the auxiliary ratio arms and d is called the yoke. The Kelvin bridge is most sensitive when A/B ratio is equal to 1. So, for most of the work done here, the bridge was worked at A/B ratio equal to 1. The details of using the bridge are discussed extensively in literature[26,11,27,28].

3.5 EXPERIMENTAL SET-UP

The following were the basic units used. The detailed procedures for the different types of experiment is given in next section.

Table 2

(L/A) Ratio of Samples for Resistance Measurement

Material used	Sample No.	Size of the wire mm	Lengths of Sample cms	(L/A) cm^{-1}
99.999% Al	1	0.85 × 0.85	58.5	8.097×10^3
	2	0.85 × 0.85	58.7	8.125×10^3
Al - 0.35 wt % Mn alloy	1	0.94 × 0.90	54.1	6.40×10^3
Al - 1.0 wt % Mn alloy	1	1.011 mm dia	57.5	7.16×10^3
	2	.86 × .84	53	7.33×10^3
	3	1.011 mm dia	48.5	6.039×10^3
	4	1.011 mm dia	43.7	5.44×10^3

3.5.1 High Temperature Furnaces (Air Furnaces)

(a) Bottom Sealed Furnaces :

Two bottom sealed furnaces were used. The inside diameter of tube was 56 mm and it was 375 mm long. The 100 mm long refractory plug closing the bottom, rested on an arbestos board. The constant temperature zone is about 75 mm in length and it is immediately above the plug. The top end of the furnaces was closed by removable refractory lid. This lid was cut in two vertical halves. A rectangular vertical groove was also cut at the cut sides of the halves to facilitate the hanging of sample in vertical position. In one of the lid halves, two 6 mm dia holes were provided to take two 6 mm dia two hole thermocouple refractory tubes. Chromel-alumel thermocouples, inserted through these holes were put at a height of about 4 cms from the inside bottom of the furnace. The coiled part of the sample rested at this height of furnace.

One of the thermocouples was connected through chromel-alumel compensating leads to a Leeds and Northrup Thermocouple Electromax Signalling 'on-off' controller, which had an accuracy of $\pm$ 0.7°C. The other thermocouple was connected to a L & N Potentiometer, which measures the furnace temperature accurately.

(b) Quenching Furnace :

This furnace was similar to the above two furnaces excepting that the bottom was open. It had a tube of 56 mm dia and of 70 cm length. The furnace was put on a raised platform, which had a big

sized hole, to let the bottom hole of the furnace freely open. The bottom hole of the furnace was closed and opened with the help of a metallic movable lid hinged to the plateform. The top lid was cut into two halves as a case of above furnaces. One half had two holes of 6 mm dia for thermocouples. This half was tightened by wires externally to fix it vertically with no movements. The other half of lid was cut horizontally, so that it did not get into furnace when put on it but just covered the hole completely. The constant temperature zone of this furnace was 50 mm long at a depth of 14.5 cms from the top of the lid of furnace. L & N electromax controller and potentiometer were used to control and measure the temperature accurately.

3.5.2 Quenching Vessel :

A steel pipe, 100 mm inside dia,and 100 cms long, having its bottom closed was taken. This was covered with asbestos cloth from all the sides except the top end. This pipe was mounted vertically on a four wheeled, movable table. A spongy packing was tightly inserted at a depth of 70 cms from the top. This quenching assembly had a total height so that the top open end of the pipe was just nearing the bottom lid of the quenching furnace, if the quenching vessel was put below it.

3.5.3 Constant Temperature Water bath in Dewar Flask :

(below room temperature). A 1500 cc beaker was put in a Dewar Flask with the help of two stands, so that its top periphery was at

the level of top periphery of the flask. A 450 watts heater was used along with a Fisher proportional controller to control the bath temperature to an accuracy of $\pm$ 0.1°C. A precision thermometer with 0.1°C graduations was used to adjust the controller. A small electric stirrer was used for stirring the bath.

3.5.4 Constant Temperature Water bath (above room temperature)

A 2000 c.c. beaker was used. A 450 watts heater was used along with the Fisher Proportional Temperature controller and with a precision thermometer of graduations 0.1°C to control the bath temperature to 70° $\pm$ 0.1°C. The small electric stirrer was used for stirring.

3.5.5 Resistance Measuring Bath :

The resistivity measurements had been made at the boiling point of liquid nitrogen (78°K) for the following reasons :

i) the quenched-in vacancies can be retained without any loss only at sufficiently low temperatures,

ii) the total resistivity of the sample decreases sharply with the decrease in the temperature of measurement. As the resistivity contribution due to the quenched-in vacancies is only a small fraction of the total resistivity of the sample, the error involved in computing the former will be considerably less if the latter is kept low.

The liquid nitrogen was taken in a one-litre, 19 cm deep Dewar Flask and the sample was inserted in it. It was ensured all the time

that the upper level of liquid nitrogen was at least 40 mm above the junction of the leads of the sample.

3.6 EXPERIMENTAL PROCEDURE :

Each sample was annealed at 600°C for 2 hrs and air cooled before any of the treatments was given to it. This was to ensure homogenisation of the wire, formation of coarse structure with low dislocation density and the formation of a thick impervious layer of alumina with no further growth of it in latter experiments.

3.6.1 Quenched-in Resistivity Measurements :

The principle of this method is to measure the extra resistivity due to quenched-in vacancies as a function of quenching tempe-ratures in pure Aluminium and in Al - 0.35 wt % Mn alloy samples. Each sample was heated in the quenching furnace, maintained at the quenching temperature, T_q, and soaked for 30 minutes. The quenching vessel had iced brine solution maintained at about 0°C. The vessel was moved, to be in alignment with the furnace hole. The botton metallic lid and top lid were opened simultaneously to allow the free fall of the sample to the quenching bath. As soon as the sample entered completely in quenching vessel, the latter was immediately moved out of the table and the sample taken out of it and transferred to ice cooled acetone in a beaker and then was immediately transferred to the Dewar flask filled with liquid Nitrogen before hand. This whole operation from opening of lid to the transfer of sample assembly to the Dewar

flask having liquid nitrogen took 5-7 seconds. The resistance of the sample was, then, measured. The sample was transferred to an air furnace maintained at 250°C via acetone. This annealing was done for 30 minutes and then the sample was taken out of the furnace and air cooled. The resistance of the sample was measured again at 78°K. The difference in resistance, ΔR, between the quenched-in state and the annealed state is due to the quenched-in vacancies. This experiment was repeated for different quenching temperatures T_q in the range 325°C to 500°C. As the retention of quenched-in vacancies in a very sensitive experiment, particularly for pure aluminium, for each temperature, at least two reading were taken for each temperature and the average value computed.

3.6.2 Isothermal Annealing at Low Temperatures :

Isochronal annealing studies on Al-0.35 wt % Mn alloy reveal that there is a recovery stage occuring around 0°C[11]. The kinetics of annealing of vacancies in this stage have been studied by quenching the alloy and pure Al samples from 445°C and employing annealing temperatures of 0°, 10°, 20° and 30°C. Each sample was heated for 1 hour at 600°C and air cooled. The sample was then quenched from 445°C after soaking for 30 minutes at 445°C as described in section 3.6.1. The as-quenched resistance was measured at liquid nitrogen temperature and then the sample was transferred to the annealing bath held at constant temperature via ice cooled acetone, maintained at temperature below the annealing temperature. After annealing for a noted time in

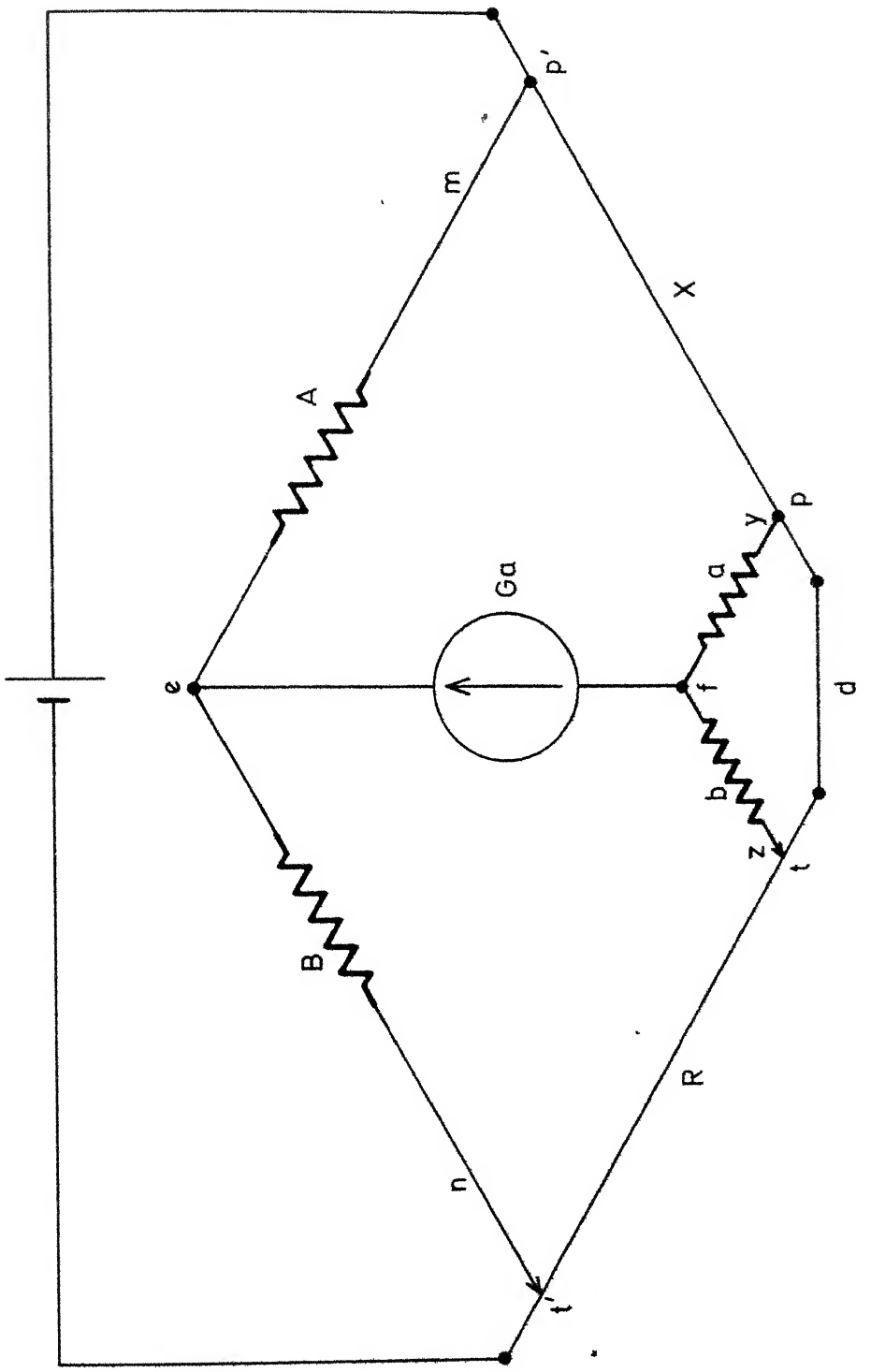

FIG. 3 Diagram of Kelvin bridge circuit

that bath, the sample was transferred to the Dewar flask having liquid nitrogen via cooled acetone. The resistance was again measured. This process was repeated for different time periods of annealing till the rate of fall of resistance approached a low value. Now, the sample was annealed in water bath kept at 70°C for 10 minutes to complete the first stage reaction and the resistance was again measured at 78°K.

3.6.3 Isothermal Annealing at High Temperature :

Isothermal annealing in the temperature range 400°C to 550°C was carried out to study the precipitation kinetics of Al-1.0 wt % Mn alloy. The sample was heated at 600°C for 36 hours for homogenising it. This was quenched in iced water and then the resistance measurement was done at 0°C. The sample was dipped in acetone cooled by ice surrounding it and when the temperature was 0°C, the resistance measurement was done. This was referred as $R_{ref.}$. Isothermal annealing was then carried out in the air furnace. The sample was taken out after known interval of time and air cooled before measuring the resistance at 0°C. The change in resistance during annealing for t minutes at a fixed temperature was given by,

$$\Delta R = R_{ref} - R_t \qquad (3.3)$$

CHAPTER 4

EXPERIMENTAL RESULTS AND DISCUSSION

4.1 QUENCHED-IN RESISTIVITY

Panseri and Federighi[21] had shown that if a sample of aluminium was quenched from an elevated temperature and then reheated for 15 minutes at 240°C, all the excess vacancies disappear and the resistivity of the sample corresponded to that of the defect-free state. So the difference in the measured value of the resistivity, $\Delta\rho$, immediately after quenching and after annealing at 240°C, corresponded to the contribution from excess vacancies retained by the quench. Similar treatment could be given to dilute Al alloys, which do not show any clustering and attendant precipitation of solutes during this treatment. Isochronal annealing studies on Al-0.35 wt % Mn alloy[11] indicated that there was no clustering in the alloy.

In order to determine the binding energy of the manganese-vacancy complex, it was first of all necessary to know the energy of formation of vacancies in pure Al. Hence quenched-in resistivity measurements were made on 99.999% pure Al. It must be emphasised that the measurement of $\Delta\rho$ is rather difficult in these samples. Even slight deformation of the samples during quenching or during subsequent handling led to abnormal values for $\Delta\rho$. In order to minimise the errors atleast three readings were taken for each quenching

temperature; the average value of the excess resistivity as a function of the quenching temperature is tabulated in Table 3. The values for $\Delta\rho$ obtained in these experiments were slightly higher than those obtained by Federighi[20] and Duckworth and Burke[19]. The temperature dependence of the as-quenched resistivity was studied by plotting log $\Delta\rho$ against 1000/T in Figure 5. The plot was linear and the equation to the straight line had been found by regression analysis to be

$$\log \Delta\rho = -3.8448 \left(\frac{1000}{T}\right) + 8.2119.$$

From this the energy of formation of a vacancy in pure Al was calculated to be 0.76 $\pm$ 0.02 eV. This value was the same as that reported by Duckworth and Burke[19] and Federighi[20]. However it was higher than the value of 0.66 eV reported by Hood et. al.[32].

The apparent energy of formation of a vacancy in the Al-0.35 wt % Mn alloy had been determined by studying the temperature dependence of the as-quenched resistivity. The results are tabulated in Table III. It is interesting to note that $\Delta\rho$ for the alloy was lower than that for the pure metal at all the temperatures. Hood et al[32] had observed that the excess resistivities arising in Al - 0.0145 wt % Mn and Al - 0.044 at % Mn alloy were higher than those in pure Al. Lahiri[11] had observed that the resistivities in Al - 0.1 wt % Mn alloy were higher than those for pure Al at temperatures below 350°C. The Arrhenius plot for log $\Delta\rho$ against 1000/Temperature for the alloy is

Table 3

Quenched-in Resistivity of pure Al (Sample No. 1) and Al-0.35 wt % Mn alloy (Sample No. 1)

I. Pure Al Sample		II. Al - 0.35 wt % Mn Sample	
$1000/T_q$ ($°K^{-1}$)	log $\Delta\rho$ ($n\Omega$-cm)	$1000/T_q$ ($°K^{-1}$)	log $\Delta\rho$ ($n\Omega$-cm)
1.6584	- .2093	1.6722	- .2877
1.6051	+ .1252	1.6051	- .0138
1.5432	+ .4897	1.6051	- .0138
1.5432	+ .4897	1.5432	+ .2151
1.4859	+ .6827	1.4859	+ .3240
1.0327	+ .8241	1.4327	+ .5649
1.3831	+ .9550	1.3831	+ .7097
1.3369	+1.1869	1.3369	+ .8273
1.2690	+1.3347	1.2937	+1.0468

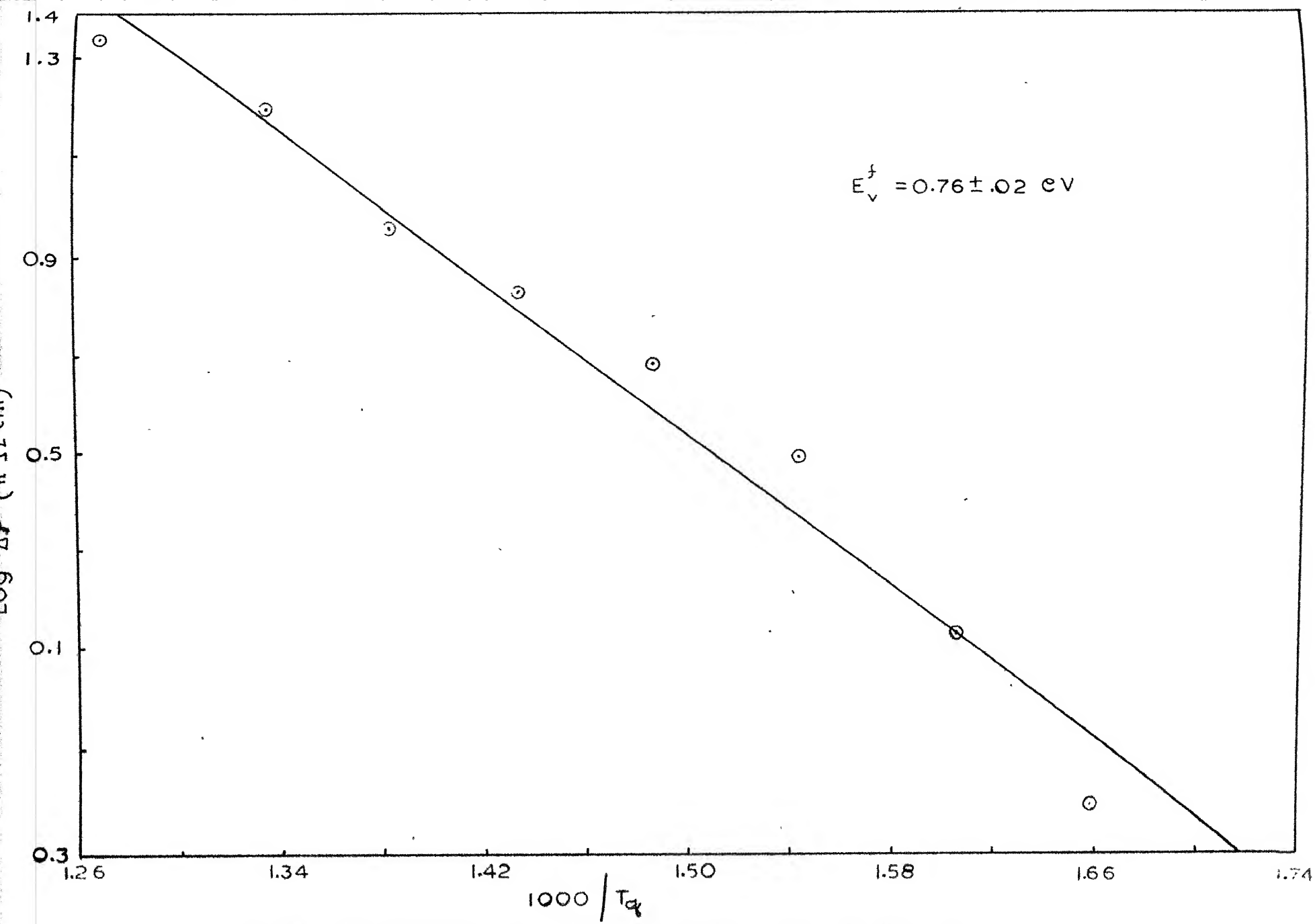

FIG 5 QUENCHED-IN RESISTIVITY OF PURE Al.

shown in Figure 6. The equation to the straight line as found out by analysis was

$$\log \Delta\rho = -3.3793 \left(\frac{1000}{T}\right) + 7.1941 .$$

From the slope of the straight line, the apparent activation energy for the formation of the vacancy in the alloy was found to be 0.67 ± 0.02 eV. For Al - 0.1 wt % Mn alloy the apparent activation energy had been found to be 0.58 ± 0. 04 eV[11].

4.2 BINDING ENERGY FROM AS-QUENCHED RESISTIVITY MEASUREMENT

The manganese-vacancy binding Energy can be calculated by equation (2.19) which is due to Duckworth and Burke[19]. This equation has an unknown term θ, which is defined as the ratio of the resistivity contribution due to an associated vacancy to that of a free vacancy.

Ramachandran and Jena[34] and Lahiri[11] had studied the effect of clustering during the quenching of aluminium alloy containing small amounts of solute atoms by extending the theoretical calculations of Doyama[36]. Reformulation of the expressions for quenched-in resistivity on the basis of clustering indicated[11] that ΔE is defined by

$$\Delta E = \frac{12\, I_o\, B_{Vi}\, \exp B_{Vi}/k\, T_q}{1-13\, I_o + 12\, I_o \exp \frac{B_{Vi}}{kT_q}}$$

This expression was similar to that of Duckworth and Burke, excepting that the term θ was absent in the numerator.

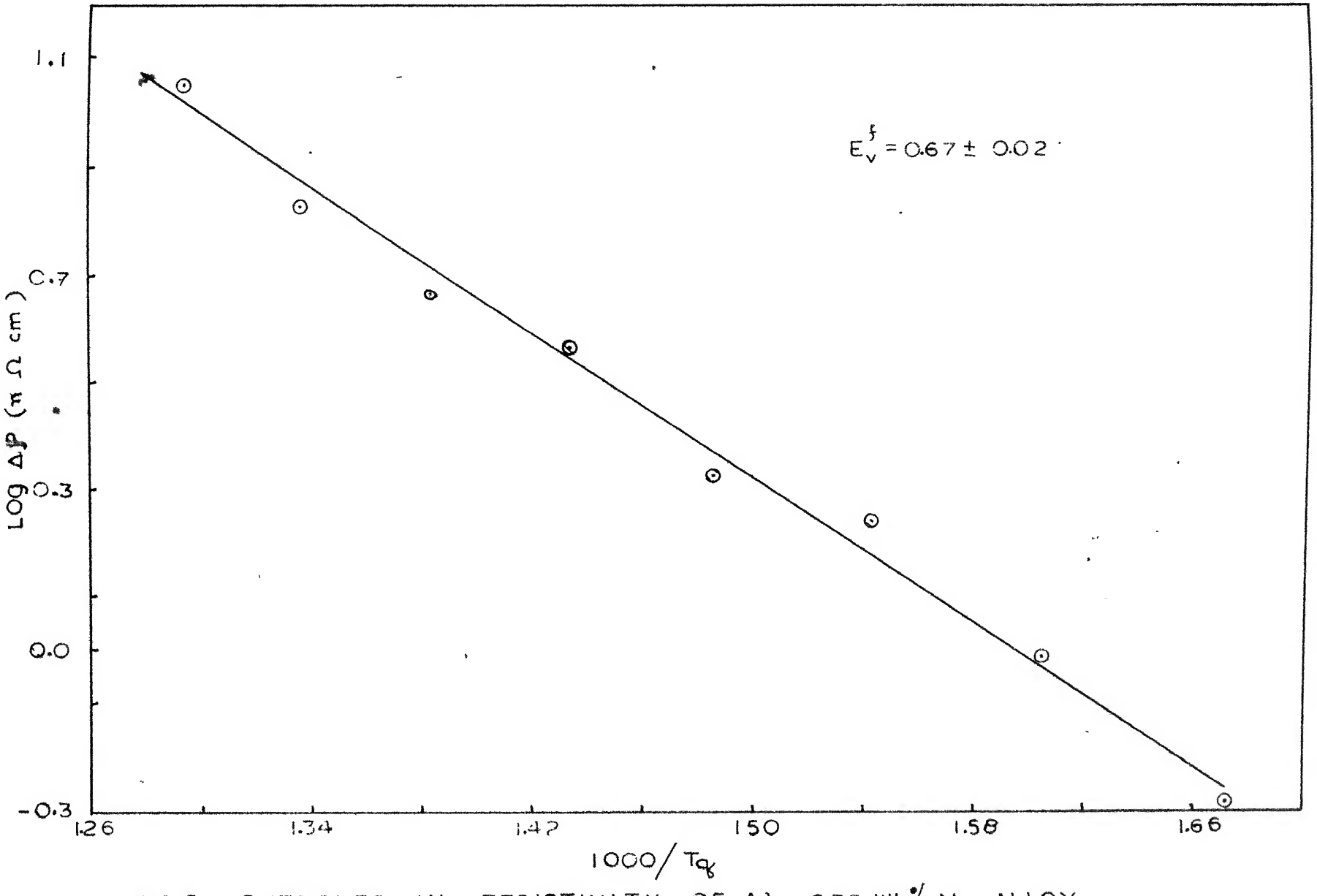

FIG 6 QUENCHED-IN RESISTIVITY OF Al - 035 Wt% Mn ALLOY

In the present investigation, E_V^f for pure Al = (0.76 ± 0.02) eV and E_V^{f*} for Al - 0.35 wt % Mn alloy = (0.67 ± 0.02) eV, so, $E_V^f - E_V^{f*} = \Delta E$ = (0.09 ± 0.03) eV. With this value of ΔE, I_o as 17.25×10^{-4} atomic fraction and taking the average quenching temperature T_q to be equal to 410°C, the equation (4.1) was satisfied with B_{Vi} equal to (0.21 eV). Lahiri[11] had reported B_{Vi} value for Al - 0.10 wt % Mn alloy to be (0.29 ± 0.04) eV, whereas Hood et al had reported it to be (0.15 ± 0.15) eV. The present value of 0.21 eV lied in between these two values.

4.3 ISOTHERMAL ANNEALING OF VACANCIES

As discussed in chapter 2, B_{Vi} can be found out by analysis of Kinetics of annealing of vacancies in pure metal and its dilute alloys as given by equation (2.35),

$$K_e = \frac{K_3}{1 + 12\, I_o \exp\left(\frac{B_{Vi}}{kT}\right)}$$

if K_3 and K_e are determined at a fixed annealing temperature, T. The equation (2.29) gives the total number of vacancies in the alloy at any time t during annealing process, which is rewritten as,

$$N = V_o' \left[1 + \left(\frac{K_1}{K_2}\right) I_o\right] \exp\left(-K_e\, t\right)$$

The excess resistivity due to presence of vacancies is

$$\Delta\rho = \rho_V V_o' \left[1 + \theta I_o \left(\frac{K_1}{K_2}\right)\right] \exp\left(-K_e\, t\right) \qquad (4.1)$$

The pre-exponential factors are constants for a constant annealing temperature. So, taking logarithm on both sides of equation (4.1), we get

$$\log (\Delta\rho) = \log c - \frac{K_e t}{2.303}) \qquad (4.2)$$

Now in the annealing experiments,

$$\Delta\rho = \rho_t - \rho_f \qquad (4.3)$$

$$\Delta\rho_o = \rho_q - \rho_f \qquad (4.4)$$

where ρ_q = Resistivity of the sample in as quenched state

ρ_t = Resistivity of the sample after annealing for t minutes

ρ_f = Resistivity of the sample after annealing for 10 minutes at 70°C at the end of isothermal annealing, which ensures the completion of first stage reaction[11,20].

$\Delta\rho_o$ is constant for an experiment. Let us substract $\log \Delta\rho_o$ from both sides of equation (4.2), we get

$$\log (\frac{\Delta\rho}{\Delta\rho_o}) = \log (\frac{c}{\Delta\rho_o}) - (\frac{K_e}{2.303})^t \qquad (4.5)$$

$$= \text{constant} - (\frac{K_e}{2.303})^t \qquad (4.6)$$

A plot of $\log (\frac{\Delta\rho}{\Delta\rho_o})$ against the time of annealing, t, can give the value of K_e. An isothermal annealing experiment, carried out on a quenched pure Al sample, will lead to the determination of K_3. The known values of K_e and K_3 can, then be used to determination of B_{Vi}.

4.3.1 Isothermal Annealing of pure Al for T_q = 445°C

The experimental procedure had been described in chapter 3. The temperature of quenching was 445°C. The annealing temperatures used were 0°, 10°, 20°, and 30°C. These temperatures were arrived at from the isochronal data of Federighi[20].

The experiments were repeated atleast twice at each annealing temperature. The results, of one set at each temperature, were tabulated in Table 4. The isothermal annealing data were also shown as plots of $\log \frac{\Delta\rho}{\Delta\rho_o}$ against time for various annealing temperatures in Figure 7. The values for the rate constant, K_3, at various temperatures were found from the slope of the linear plots. The average values of K_3 were shown in Table 4.

The temperature dependence of the rate constant had been shown as a plot of $\log K_3$ against 1000/K° in Figure 8. The linear slope proved that the annealing process obeys the first order kinetics and so the activation energy of 0.65 eV can be identified with the migration energy of a single vacancy in Al. This value of 0.65 eV was in good agreement with the value of 0.67 eV as reported by Lahiri[11] and 0.60 - 0.65 eV as reported by Federighi[20].

4.3.2 Isothermal Annealing of Al - 0.35 wt % Mn alloy for 445°C.

The experimental procedure had been described in chapter 3. To decide about the temperatures of annealing, the isochronal data

Table 4

Isothermal annealing of pure Al (Sample 1)

Quenching Temperature = 445 ± 1°c

I. Annealing Temp = 0.0°c

Annealing Time Minutes	$\frac{\Delta\rho}{\Delta\rho_o}$	$\log\left(\frac{\Delta\rho}{\Delta\rho_o}\right)$
0.0	1.0000	0.0000
2.5	0.8947	-0.0483
7.5	0.7763	-0.1100
12.5	0.6710	-0.1733
17.5	0.6447	-0.1906
25	0.5000	-0.3010

K_3 at 0°c = .0245016 min^{-1}

II. Annealing Temp = 10°c

Annealing Time Minutes	$\frac{\Delta\rho}{\Delta\rho_o}$	$\log\left(\frac{\Delta\rho}{\Delta\rho_o}\right)$
0	1.0000	0.0000
1	0.8235	-0.0843
3	0.7647	-0.1165
7	0.5294	-0.2762
13	0.3823	-0.4175
21	0.1764	-0.7533
31	0.0816	-0.0882

K_3 at 10°c = .064357 min^{-1}

III. Annealing Temp = 20°c

Annealing Time Minutes	$\frac{\Delta\rho}{\Delta\rho_o}$	$\log\left(\frac{\Delta\rho}{\Delta\rho_o}\right)$
0.0	1.0000	0.0000
0.5	0.8775	-0.0568
1.5	0.8571	-0.0670
3.5	0.5102	-0.2923
6.5	0.2653	-0.5763
10.5	0.1836	-0.7360
15.5	0.0816	-1.0882

K_3 at 20°c = .16256 min^{-1}

IV Annealing Temp = 30°c

Annealing Time Minutes	$\frac{\Delta\rho}{\Delta\rho_o}$	$\log\left(\frac{\Delta\rho}{\Delta\rho_o}\right)$
0.0	1.0000	0.0000
1.0	0.7441	-0.1284
2.0	0.5232	-0.3217
3.5	0.3023	-0.5196
5.0	0.1651	-0.7822
7.5	0.6720	-1.1421

K_3 at 30°c = .383510 min^{-1}

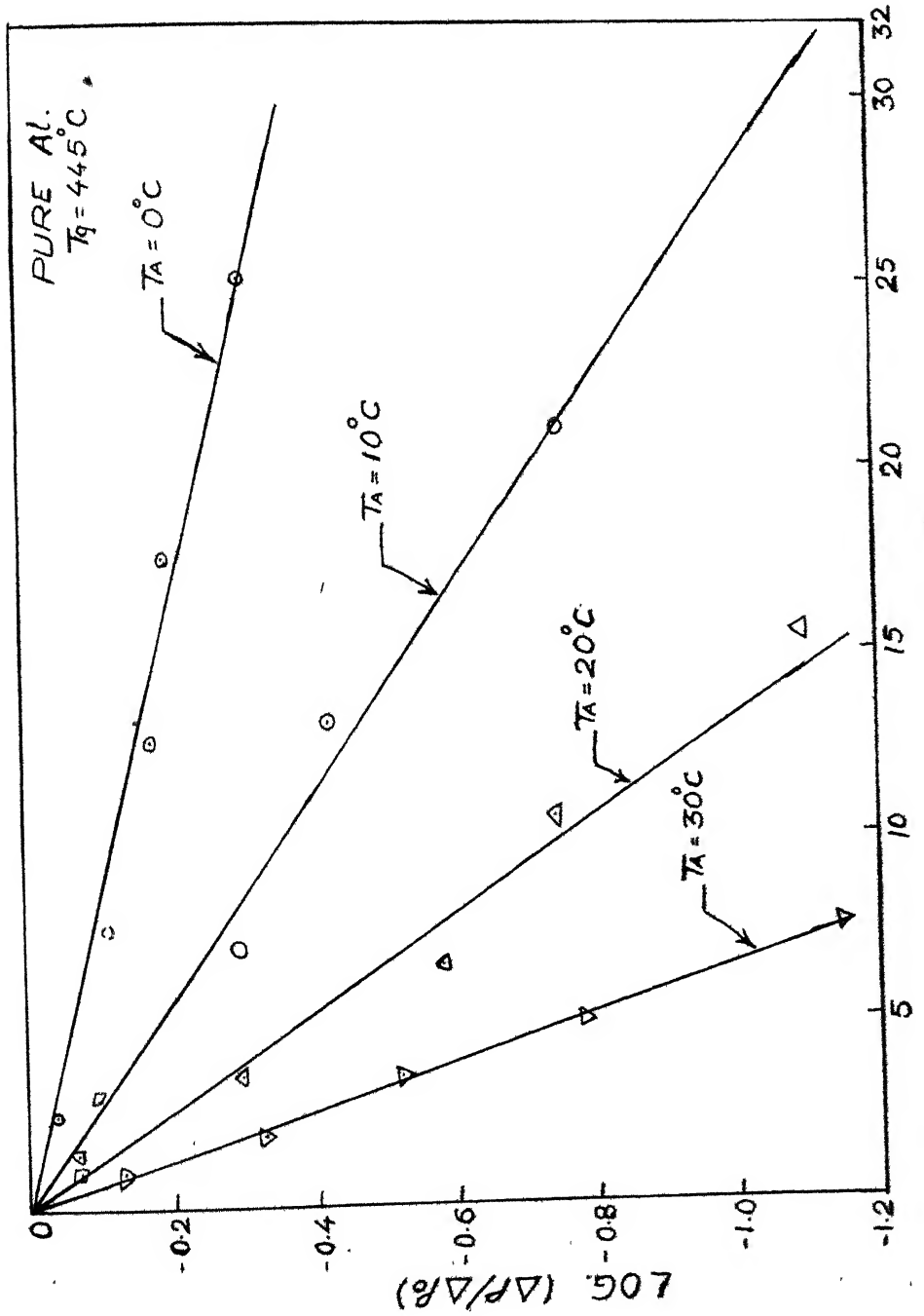

FIG. 7 ISOTHERMAL ANNEALING OF PURE Al.

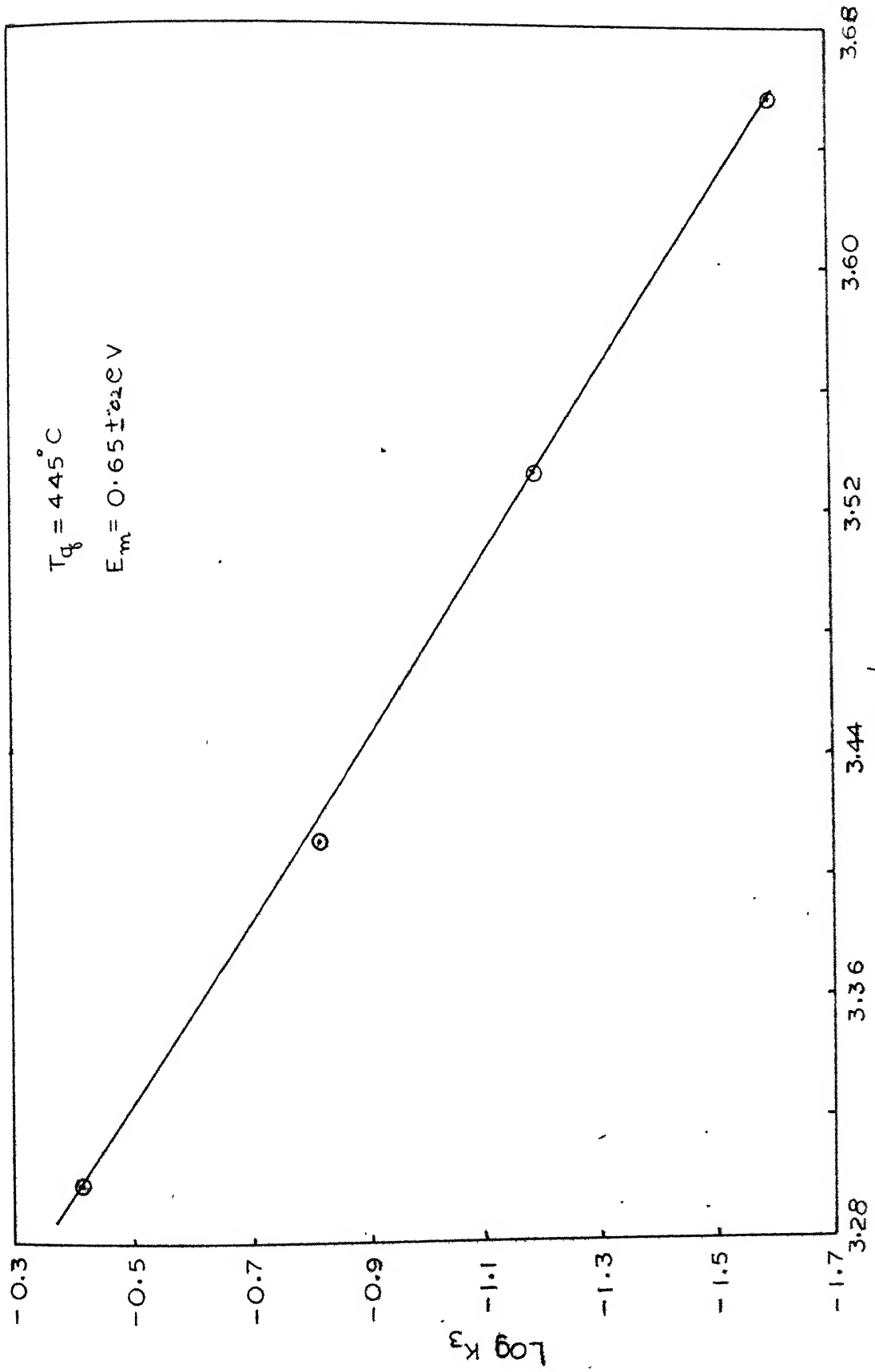

FIG 8 RELATIONSHIP BETWEEN LOG K AND ANNEALING TEMPERATUPE T_A

of Lahiri[11] for Al - 0.35 wt % Mn alloy, as shown as plot in Figure 9, was analysed. The recovery stage appeared to take place in range 0° to 40°C. So, the isothermal annealing temperatures chosen were 0°, 10°, 20° and 30°C. As the higher temperature of quenching (620°C) used by Lahiri[11], might cause complications, such as formation of clustering, divacancies, etc., 445°C was used as the quenching temperature in this investigation.

The experiment was repeated atleast twice at each temperature of annealing. The results of one set of data were tabulated in table 5. The plots of log $(\frac{\Delta\rho}{\Delta\rho_o})$ against annealing time for different sets for one temperature were plotted separately and then the average curves were drawn. Figure (10) showed the plots of various sets of data for one temperature and the average curve had been drawn there in. Such average curves for different annealing temperatures had been plotted in Figure (11). It was clear that the plot of log $(\Delta\rho/\Delta\rho_o)$ against time was made up of two parts. So, the vacancy elimination reaction, in this alloy, did not obey Ist order kinetics. This was likely to be due to the presence of di-vacancies, which were known to anneal out at a faster rate than mono-vacancies, or due to solute-solute clusters. Duckworth and Burke also got such deviation from the first order kinetics while investigating Al-Mg alloys containing .0053 to 0.0482 at % Mg quenched from 420°C. Lahiri[11] also, got such deviation from the first order kinetics while investigating Al-0.35 wt % Mn alloy quenched from 445°C. As a linear relationship existed during

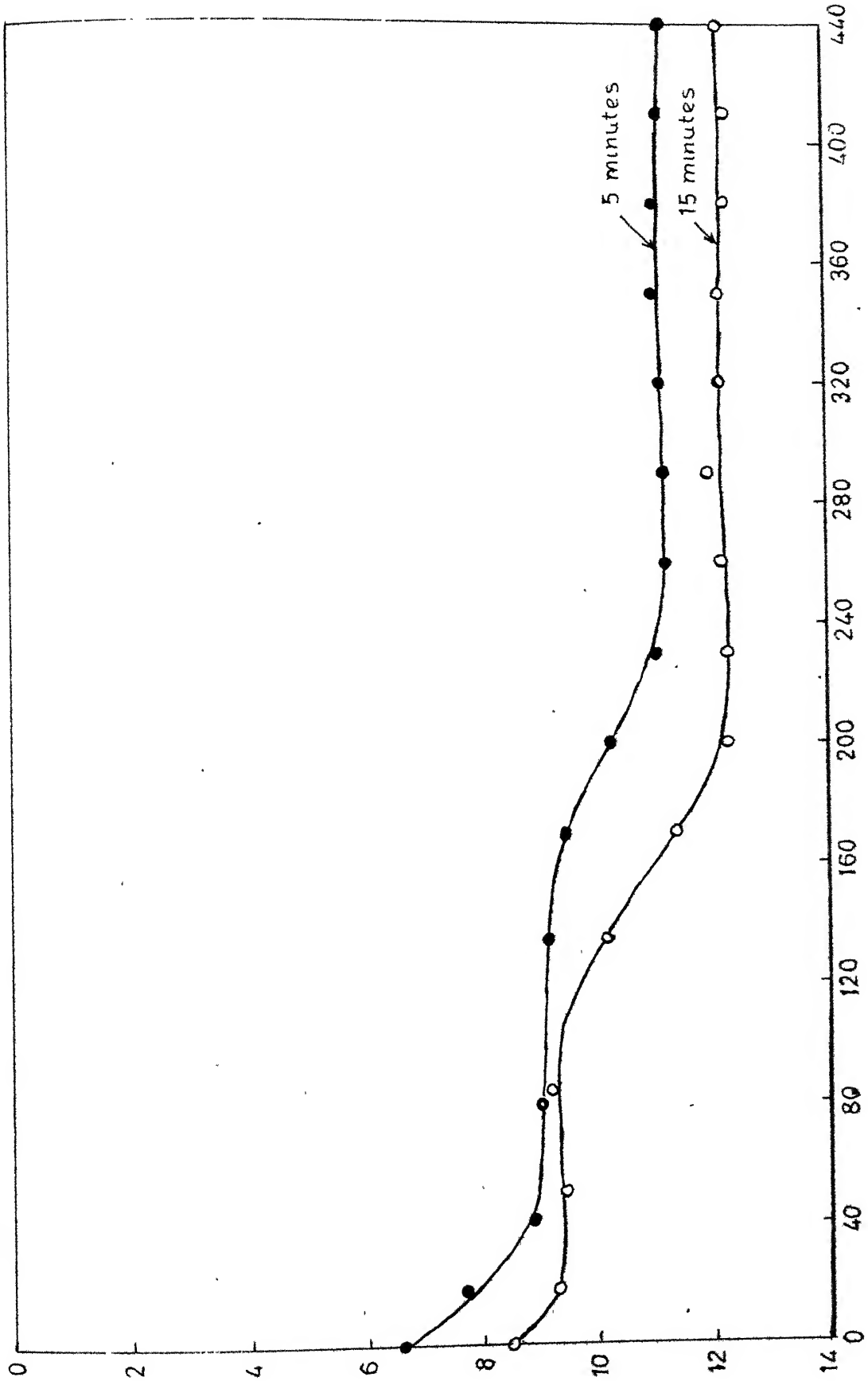

Fig.4 Isochronal annealing of quenched Al-0.35 wt% Mn alloy.

Table 5

Isothermal annealing of Al-0.35 wt % Mn alloy (Sample No. 1)

Quenching Temperature = 445 ± 1°C

I. Annealing Temp = 0.0°C

Annealing Time Minutes	$\frac{\Delta\rho}{\Delta\rho_o}$	$\log\left(\frac{\Delta\rho}{\Delta\rho_o}\right)$
0	1.0000	0.0000
2.5	0.9815	0.0082
7.5	0.7777	0.1092
14.5	0.7593	0.1196
39.5	0.5370	0.2700
54.5	0.3888	0.4102

II. Annealing Temp = 10°C

Annealing Time Minutes	$\frac{\Delta\rho}{\Delta\rho_o}$	$\log\left(\frac{\Delta\rho}{\Delta\rho_o}\right)$
0	1.0000	0.0000
1.5	0.925	-0.0338
4.5	0.825	-0.0835
9.0	0.700	-0.1549
15.0	0.625	-0.2041
22.5	0.475	-0.3233
32.5	0.450	-0.3468

III. Annealing Temp = 20°C

Annealing Time Minutes	$\frac{\Delta\rho}{\Delta\rho_o}$	$\log\left(\frac{\Delta\rho}{\Delta\rho_o}\right)$
0	1.000	0.0000
0.5	0.8235	-0.0843
1.5	0.7059	-0.1512
3.5	0.6471	-0.1890
6.5	0.5882	-0.2304
11.5	0.4706	-0.3273
18.5	0.3529	-0.4522

IV. Annealing Temp = 30°C

Annealing Time Minutes	$\frac{\Delta\rho}{\Delta\rho_o}$	$\log\left(\frac{\Delta\rho}{\Delta\rho_o}\right)$
0	0.1000	0.0000
0.5	0.8369	-0.0773
1.5	0.7162	-0.1450
3.0	0.6180	-0.2090
5.0	0.4851	-0.3142
7.5	0.3861	-0.4133
10.5	0.3043	-0.5166

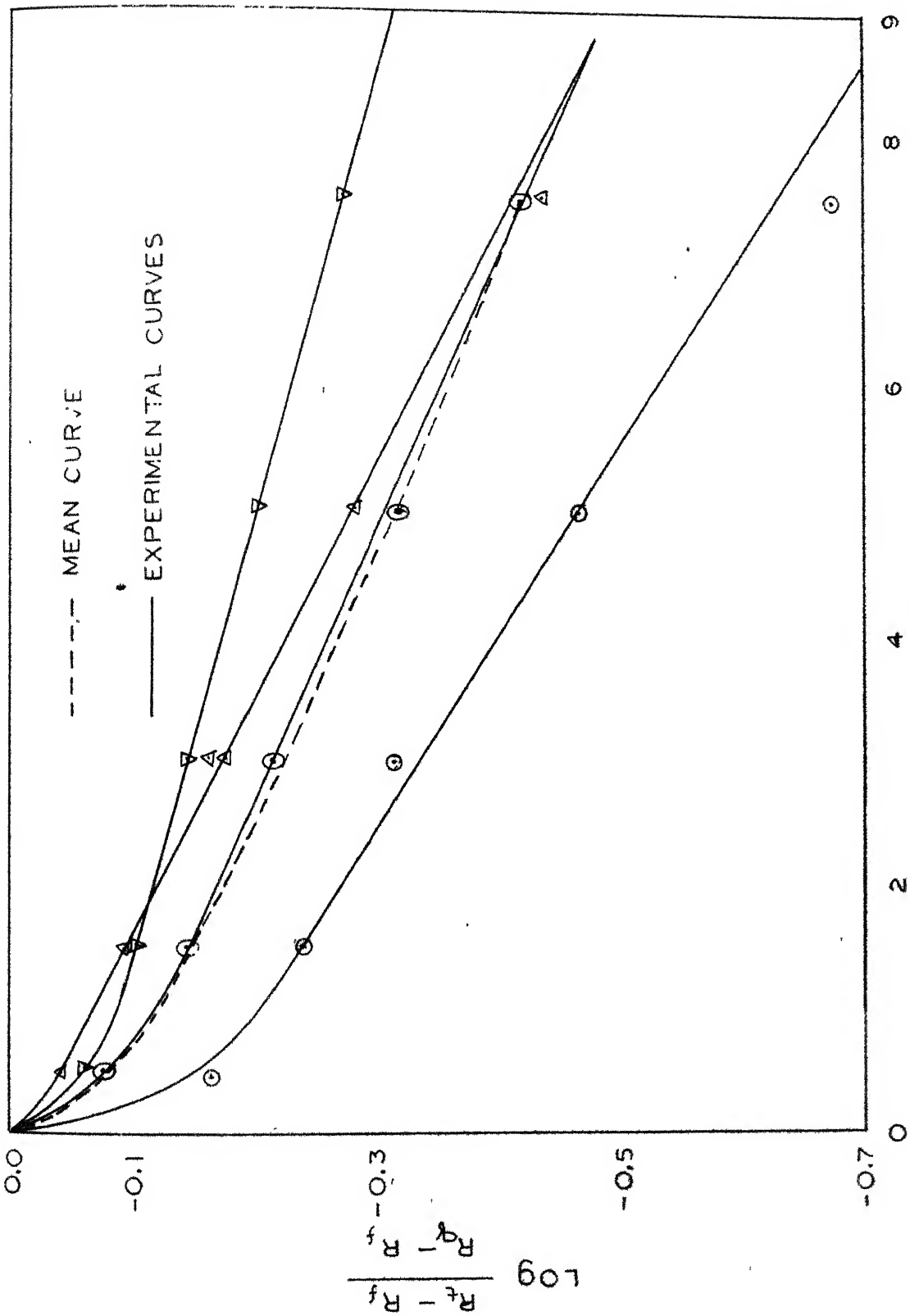

FIG 10 ISOTHERMAL ANNEALING OF AL 0.35 Wt% Mn ALLOY AT 30°C

FIG 11 ISOTHERMAL ANNEALING OF AL-0.35 wt% M[illegible] ALLOY

the later part of Annealing, this portion had been used by the above research workers to get the value of K_e. From this value of K_e, Lahiri[11] determined the average value of Binding energy to be (0.10 ± 0.4) eV. Calculations were made to get B_{Vi} values for the present investigation on similar principles and results are : B_{Vi} = 0.15 eV at 303°K, 0.12 eV at 293°K, 0.11 eV at 283°K and .08 eV at 273°K. The average value was $(0.12 \pm .03)$ eV. This was an arbitrary method for calculating B_{Vi}. There appeared to be no justification for using the later part of the curve to calculate the value of the binding energy.

However, another method can be used to calculate the binding energy. The kinetics of annealing of dilute alloys in the presence of mono-and di-vacancies had been expressed in terms of equations (2.36) to (2.39). But before solving them, we were supposed to know the terms ρ_{Vi} and ρ_{2V}, i.e. the resistivity contributions due to complex and due to a divacancy. But if we assumed $\rho_{2V} = 2\rho_V$ and $\rho_{Vi} = \rho_V$, then these equations could be solved. Ramachandran[30] solved these equations in an IBM 7044 digital computer for a number of value of B_{Vi} for isothermal annealing at 273°, 283°, 293° and 303°K. The relevant data used for calculations are given in Appendix I. We find that computer gave the variations of single vacancy concentrations, di-vacancy concentrations, complex concentrations and total vacancy concentrations with time. Plots could be made for the variation of total vacancy concentrations with the time. The experimentally produced

data could be compared with these plots. The figures (12), (13), (14) and (15) showed the comparison of these curves. The curves matched well for the data of two temperatures, (273° and 283°K) each giving a value of Binding energy as 0.10 eV. The experimental curve for the temperature 293°K, cut the computer data curve. This behaviour could not be explained, however, most of the experimental points appeared to surround the plot plotted for binding energy of value 0.10 eV. The experimental curve for the annealing temperature 303°K, appeared to follow the path as if it had a value of 0.10 eV, as shown in the Figure (15), the computer data for which was not available.

Table 7

Determined values of Binding energy by comparison means

Annealing Temp K°	B_V- Mn eV
273	0.10
283	0.10
293	0.10
303	0.10
Average	0.10

4.4 COMPARISON OF B_{V-Mn} VALUES

The thermodynamic method gave a value of B_{V-Mn} as $(0.21 \pm .03)$ eV. The isothermal Annealing data gave a value of 0.10 eV. Similar, large

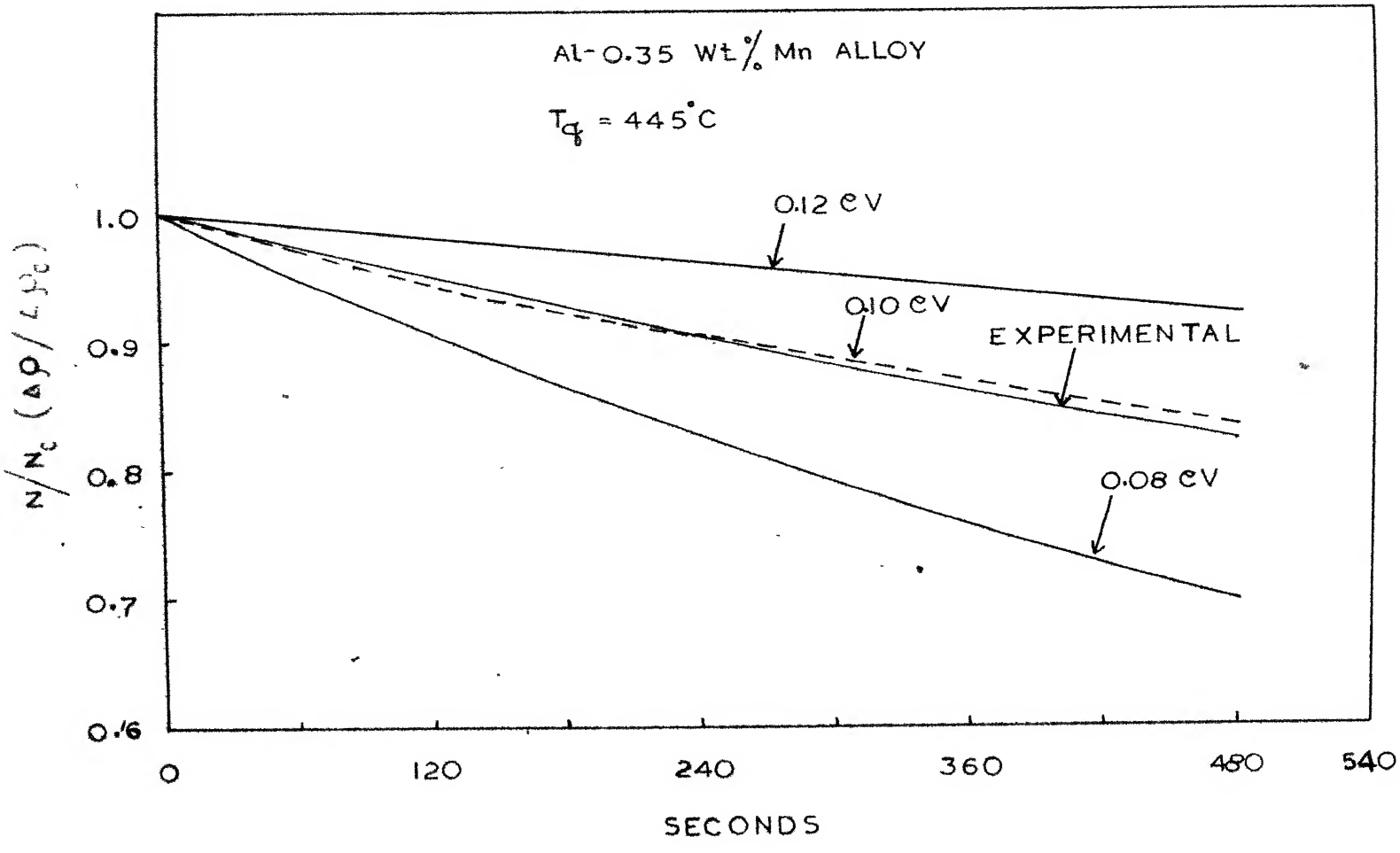

FIG 12 COMPARISON OF CALCULATED AND EXPERIMENTAL DATA FOR T_A = 273°K

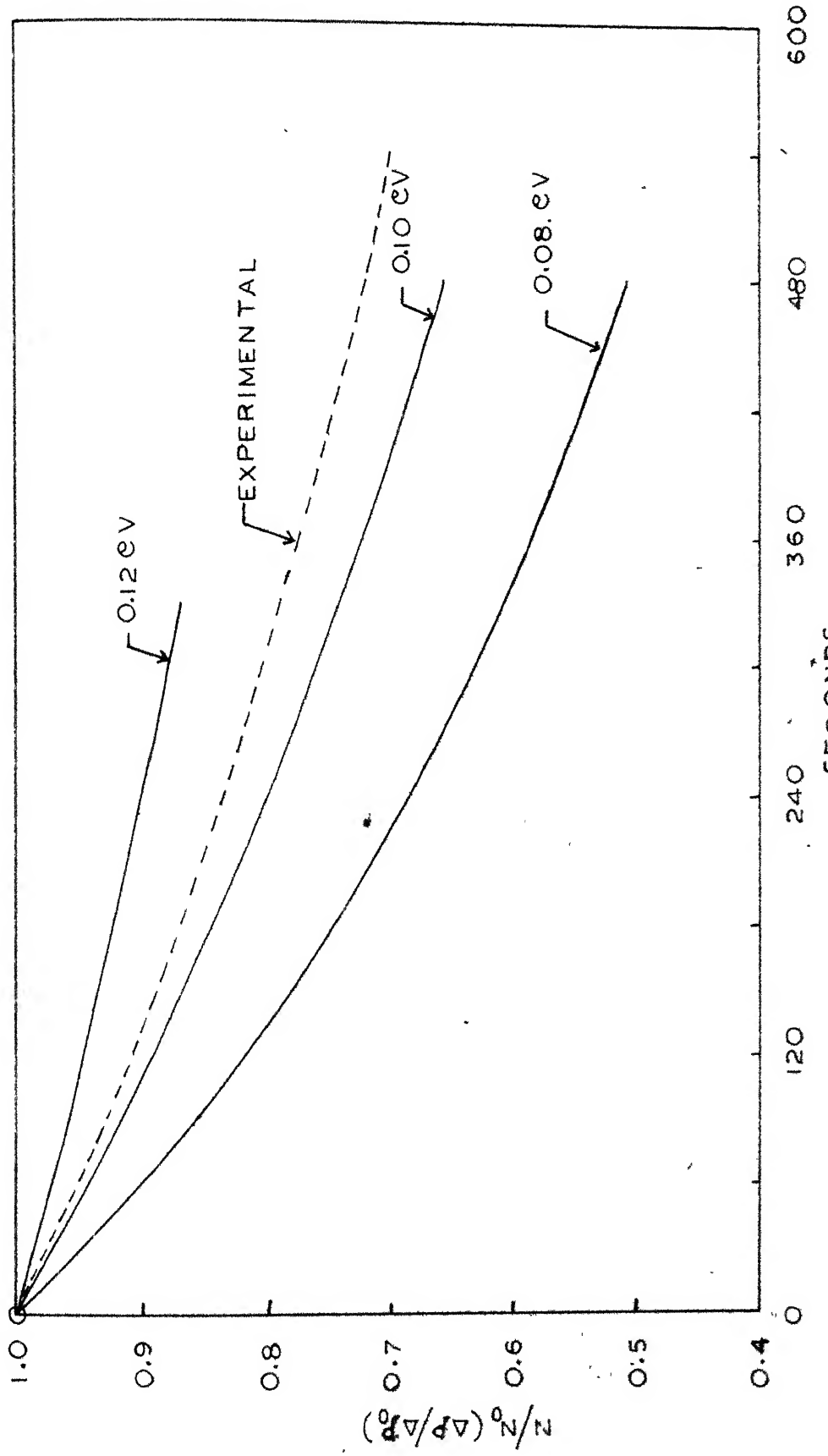

FIG 13 COMPARISON OF CALCULATED AND EXPERIMENTAL DATA FOR $T_A = 283^\circ K$

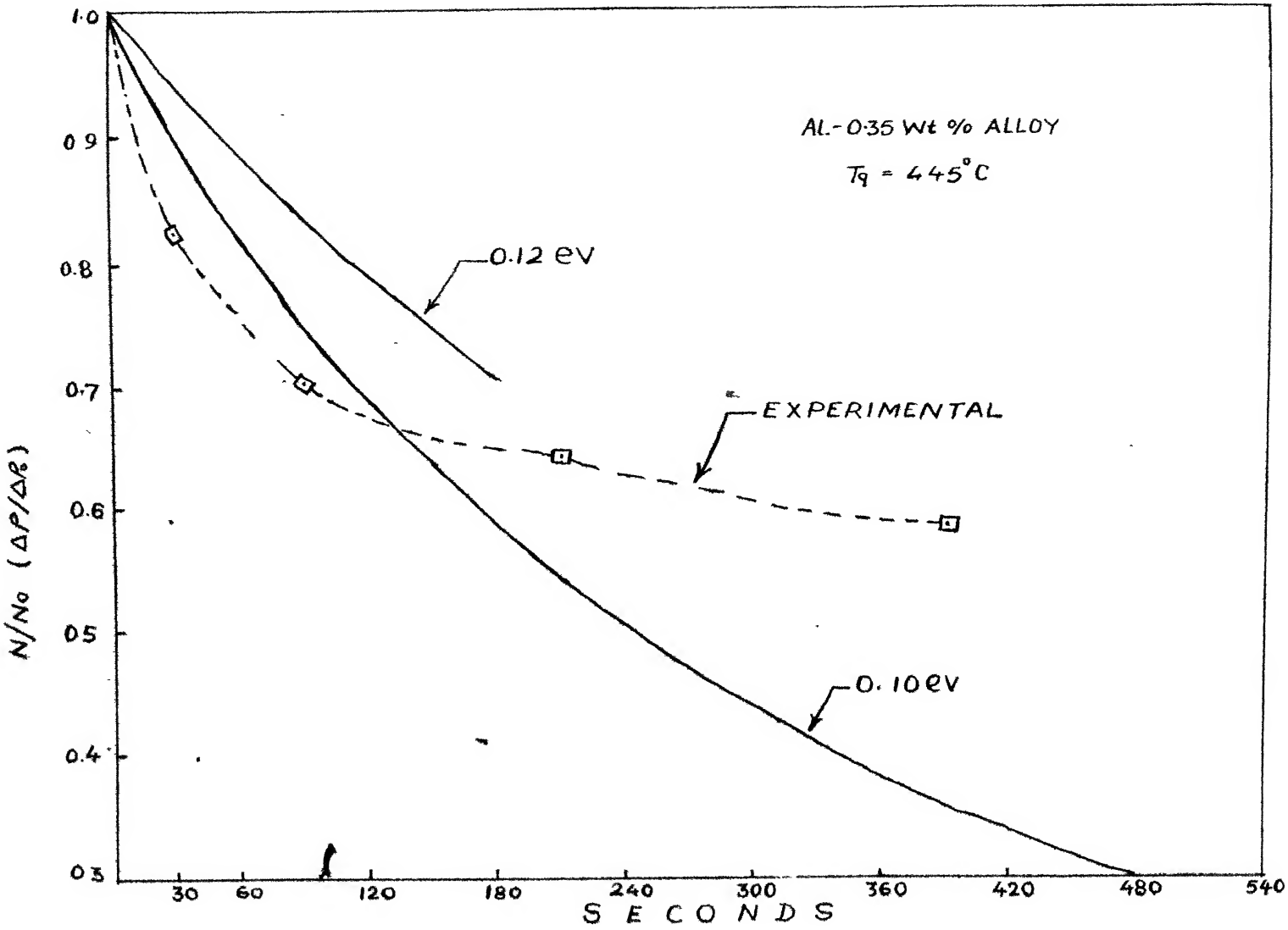

FIG 14 COMPARISON OF CALCULATED & EXPERIMENTAL DATA FOR T_A = 293° K

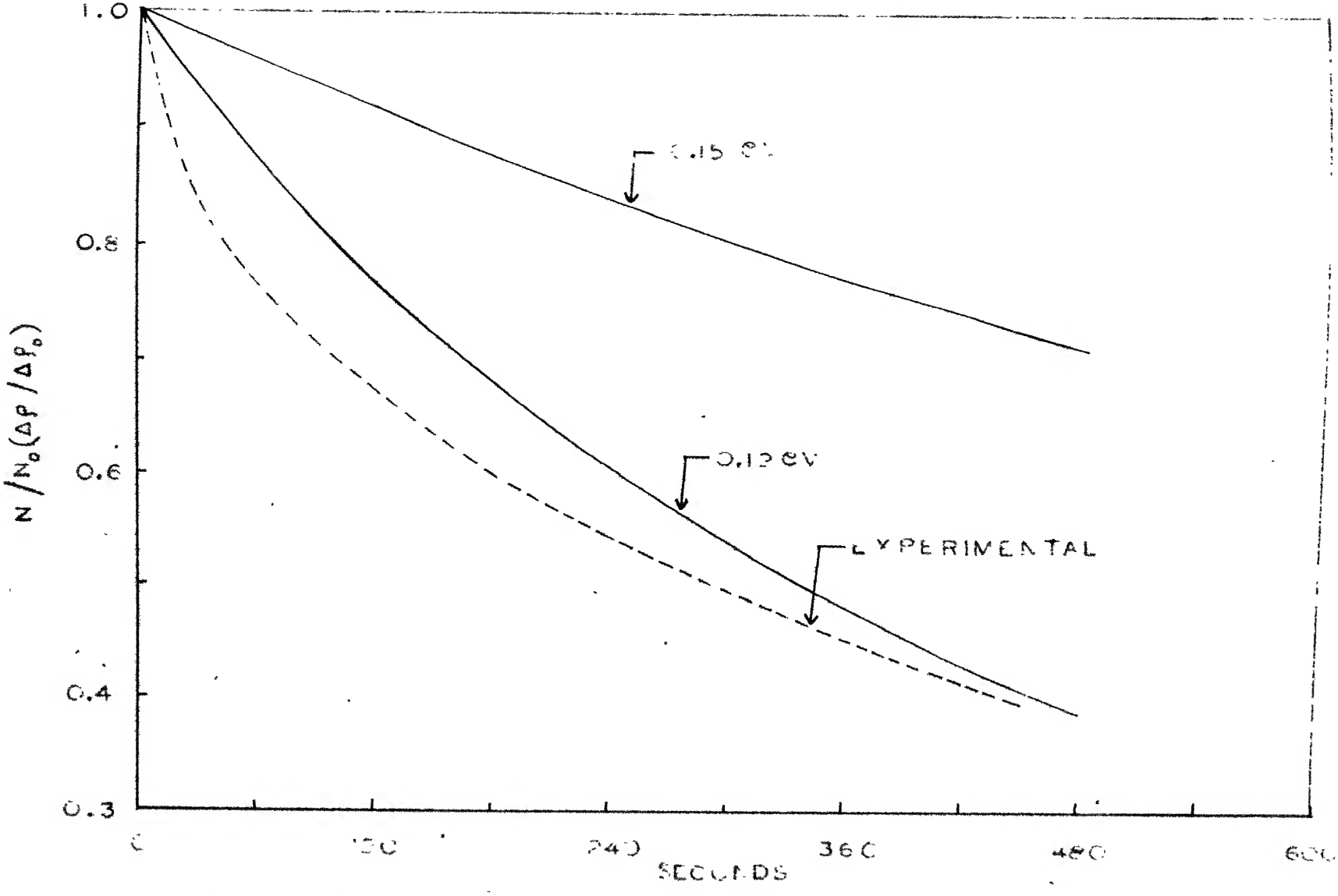

FIG 15 COMPARISON OF CALCULATED AND EXPERIMENTAL DATA FOR

$T_A = 303$

The kinetic data can be treated as more reliable. The value of 0.10 eV obtained for the binding energy is in good agreement with that obtained by Lahiri[11]. While the discrepancy in the binding energy valueis appreciable in the values obtained by Lahiri by the kinetic and thermodynamic methods (0.10 and 0.29 eV respectively), the present results are slightly better (0.10 eV and 0.21 eV respectively).

4.5. Isothermal Precipitation in Al-1.0 wt % Mn Alloy :

The first stage in precipitation studies involves the homogenisation of the two phase alloy. The limited studies on precipitation in the Al-Mn system[11] indicate that precipitation is very sluggish in this system. To ensure that the Al-1% Mn alloy is completely homogenised before quenching, the alloy was heated at 600°C for varying times, quenched-in water and the resistivity measured. The variation of the resistivity with homogenising time is shown in Figure 16. From the figure it is clear that homogenising is complete only after 36 hours.

The completely homogenised alloy is quenched in water and then artificially aged in the temperature range 400to 550°C and the resistivities measured as a function of ageing time. The results are shown in Appendix III and are plotted as the relationship between $\Delta\rho$ against logarithm of annealing time in Figure 17. Logarithmic time scale has been chosen to accomodate large times of ageing like 20,000 minutes. It is clear from the figure that the rate of annealing decreases gradually with increase in time. For a fixed time $\Delta\rho$ is for more with increase in annealing temperature. The precipitation reaction has the maximum rate at 550°C, this is in good agreement with the

results of Ferrari et al[9] who have observed the maximum rate at 575°C. However while Ferrari et al observe that the supersaturated solid solution decomposed in less than 300 hours to the equilibrium phases, for temperature above 525°C, the present results indicate that equilibrium has not been reached even after ageing for 42 days at 500°C. This is clearly indicative of the sluggish precipitation characteristics in the Al-Mn system.

In order to find out the amount of solute remaining in solution after varying times of ageing of the supersaturated alloys, a master curve was first established between the electrical resistivity and % Mn in solution in Al. The resistivities of pure Al and a series of Al-Mn alloys containing 0.1, 0.35 and 1.0% Mn have been quenched from 600°C into water at room temperature have been measured at 0°C. Figure 18 shows a plot of resistivity as a function of Mn composition

Table 10

Amount of solute in solid solution for different annealing times in Al-1.0 wt % Mn alloy quenched from 600°C as a function of precipitation temperature

Annealing Temp °C	% Mn in solid solution after annealing for time, minutes				
	480	1560	4700	8700	18500
400°	0.9950	.9900	.9825	.9725	.9550
450°	0.9800	.9670	.9620	.9350	.8800
500°	0.9750	.9650	.9450	.9050	.8250
550°	0.9700	.9550	.9250	.8950	.8150

The change in resistivities at each temperature of isothermal annealing after 480, 1560, 4700, 8700 and 18500 minutes was noted and these were used along with Figure 18 to determine percentage Mn remaining in solid solution. The results are shown in Table 10.

The decomposition characteristics of quenched Al-0.35 wt % Mn alloy have been studied at 450°C. Even after 20 hours of annealing no change in resistivity could be detected.

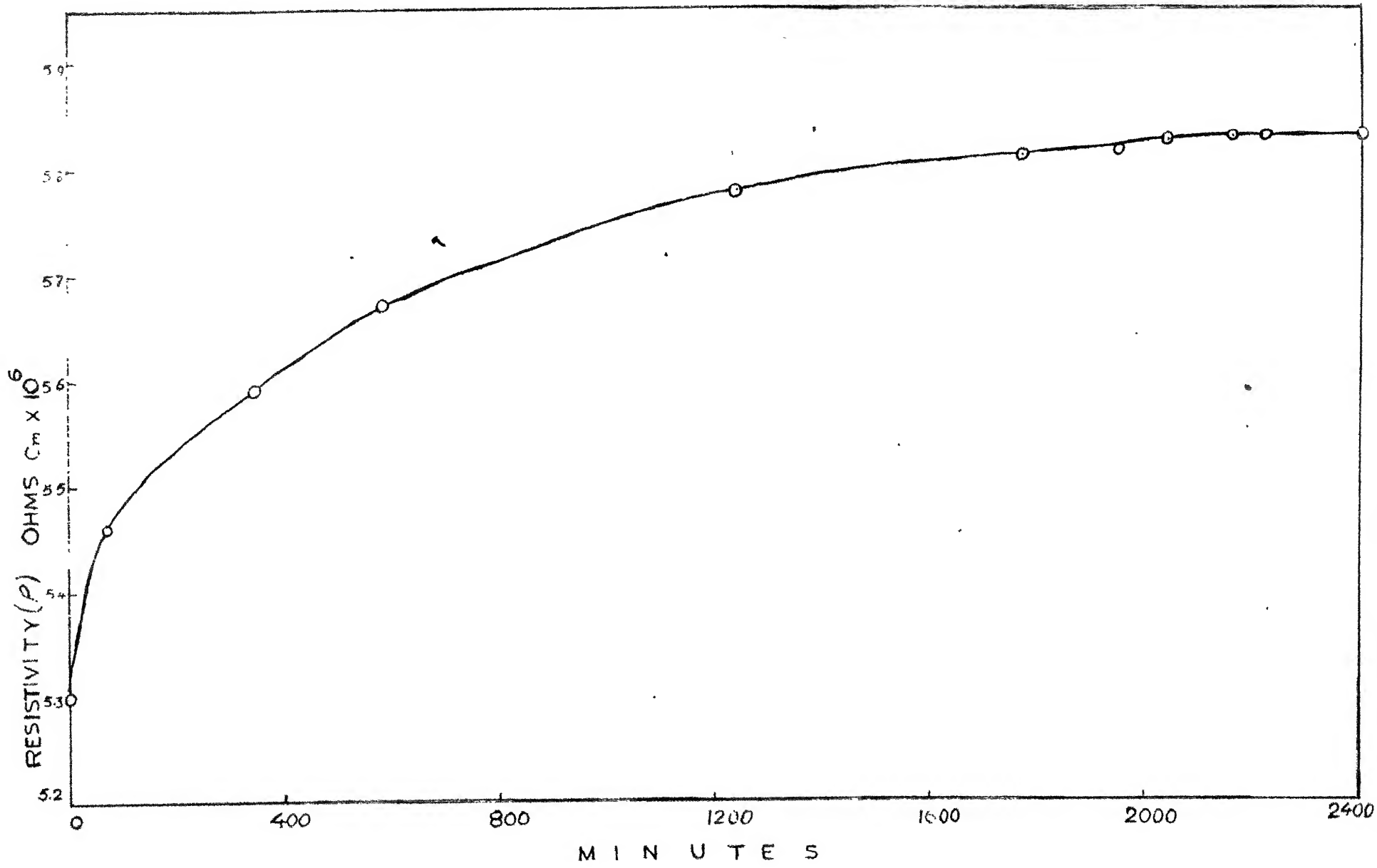

FIG. 16 HOMOGENISING PERIOD FOR THE Al.-1.0 Wt. % Mn. ALLOY

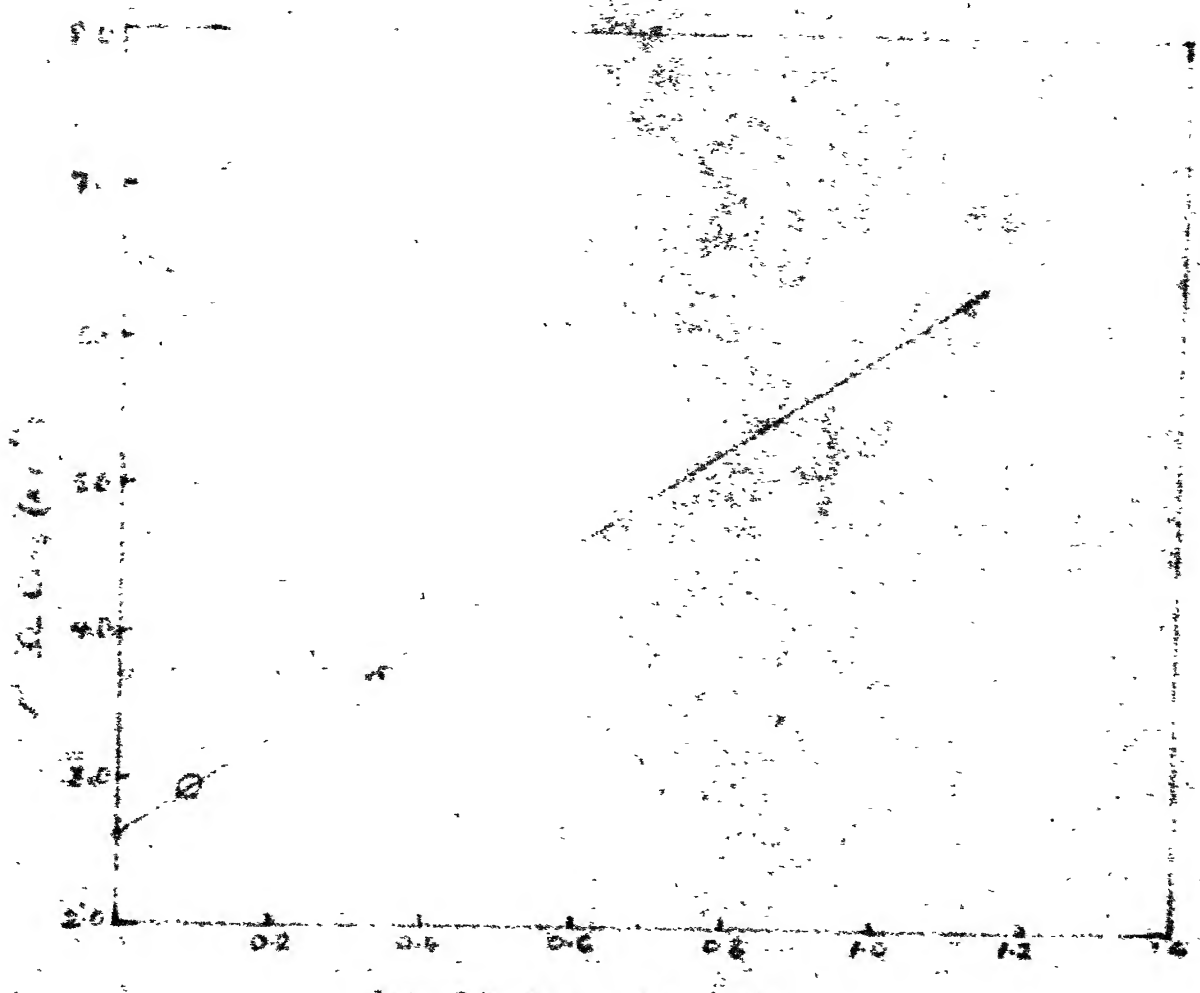

FIG 16 VARIATION OF RESISTIVITY WITH COMPOSITION IN Al Mn ALLOYS

CHAPTER 5

CONCLUSIONS

The following conclusions can be drawn from the present investigation.

(1) The activation energy for the formation of vacancy in pure Al and in Al - 0.35 wt % Mn alloy were 0.76 ± .02 eV and 0.67 ± 0.02 eV respectively.

(2) The manganese-vacancy binding energy in Al, determined from the difference in the activation energy for the formation of vacancy in pure Al and Al-0.35 wt % Mn alloy was (0.21 ± 0.3) eV.

(3) From the quenched-in resistivity measurements, it was found that the extra-resistivity obtained by quenching was smaller for Al - 0.35 wt % Mn than for pure Al for all the temperatures suggesting that the value of $\theta < 1$.

(4) The isothermal vacancy annealing in pure Al, quenched from 445°C and annealed in the temperature range 0° to 30°C, followed a Ist order kinetics.

(5) The migration energy for the motion of vacancy by analysing the data of pure Al was found to be 0.65 eV.

(6) The isothermal vacancy annealing in Al - 0.35 wt % Mn alloy quenched from 445°C did not follow a first order kinetics as evident from the nonlinear nature of the curve.

(7) The linear portion of the isothermal annealing curves for the Al - 0.35 wt % Mn alloy was used to find out the B_{Vi}, the average value of which was $(0.12 \pm .03)$ eV.

(8) The isothermal annealing data for the Al-0.35 wt % Mn alloy was compared with the theoretical computer data which had taken care of annealing of divacancies also. The matching of these data, gave Binding energy value as 0.10 eV.

(9) Considering the probable errors in the determination of B_{Vi} by both the techniques, the value obtained by the kinetic method was more reliable and this value might be taken as 0.10 eV.

(10) No evidence of precipitation was obtained when supersaturated Al - 0.35 wt % Mn alloy was annealed for 20 hrs at 450°C.

(11) The isothermal precipitation of Al - 1.0 wt % Mn alloy in the temperature range 400°C to 550°C indicated that the precipitation reaction was very sluggish and the precipitation did not go to completion even after annealing for 42 days at 500°C.

REFERENCES

1. A.C. Demask and G.J. Diones, "Point Defects in Metals", (Gordan and Breach, New York), 1963.

2. R.P. Johnson, Phys. Rev. 56, 814 (1939).

3. W.M. Lomer, "Vacancies and other Point Defects in Metals and Alloys", Institute of Metals, 79(1958).

4. C. Panseri and T. Federighi, Acta Met. 8, 217 (1960).

5. D. Turnbull, H.S. Rosenbaum and H.N. Treaftes, Acta Met. 8, 277 (1960).

6. A.J. Perry and K.M. Entwistle, J. Inst. Metals 96, 344 (1968).

7. H.S. Rosenbaum and D. Turnbull, Acta Met. 6, 653 (1958).

8. E. Nes, S.A. Naess and R. Hoier, Z. Metallk, 63 (1972) 248.

9. A Ferrari, P. Fiorini and F. Gatto, Acta Met. 15, 1073 (1967).

10. K.S. Raman, E.S.D. Dass and K.I. Kasu, J. Material Science 6, 1367 (1971).

11. D.P. Lahiri, Ph.D. Thesis, I.I.T., Kanpur (1973).

12. J. Burke, J. Less-common Metals, 28, 441 (1972).

13. J.J. Jackson and J.S. Koehler, Bull. Am. Phys. Soc. 5, 154 (1960).

14. J.S. Koehler and C. Lund, "Lattice Defects in Quenched Metals", (Academic Press, p. 1 (1965).

15. M. Kiritani, J. Phys. Soc. Japan 19, 618 (1964).

16. M, Doyama, "Lattice Defects in Quenched Metals", p. 167 (1965).

17. J.J. Jackson, Acta Met. 11, 1245 (1963).

18. G. Borelius & J.S. Koehler, Phys. Rev. 107, 1493 (1957).

19. F.C. Duckworth and J. Burke, Phil Mag. 14 473 (1966).

20. T. Federighi, "Lattice Defects in Quenched Metals" (Academic Press), p. 217 (1965).

21. C. Panseri and T. Federighi, Phil. Mag. 14, 473 (1966).

22. T.R. Ramachandran, Ph.D. Thesis, University of Wales (1969).

23. J. Burke and T.R. Ramachandran, Metal Science, J., 5, 223 (1971).

24. K.P. Chik, "Vacancies and Interstitials in Metals". (North-Holland Publishing Co., Amsterdam), 183, (1969).

25. J. Burke, "The Kinetics of Phase Transformations in Metals", (Pergamon Press, Oxford), 1965.

26. "Notes on the Kelvin bridge" by Leads and Northrup Company, Philadelphia, U.S.A., p. 6 (1961).

27. G.T. Meaden, "Electrical Resistance of Metals", (Plenum Press, New York), p. 147 (1965).

28. F.H. Harris, "Electrical measurements", (John Wiley, New York), p. 264 (1962).

29. F.C. Duckworth and J. Burke, Britt. J. Appl. Phys. 18, 1071 (1967).

30. T.R. Ramachandran, Unpublished work (1973).

31. A.J. Perry & W.J. Plumbridge, Phil. Mag. 25, 139, (1972).

32. G.M. Hood, A.F. Quennoville, R.J. Schults and M.L. Swanson, Crystal lattice defects, 2, 243 (1971).

33. K. Little, G.V. Raynor & W. Hume Rothery, J. Inst. Metals 73, 83 (1946).

34. T.R. Ramachandran and A.K. Jena, Trans. Ind. Inst. Metals, 27 (50) 303 (1974).

36. M. Doyama, Phys. Rev. 148, 681 (1966).

37. A. Ferrari, P. Fiorini, & F. Gatts, Alumino, 223-229, 35(15) 1966.

APPENDIX I

Table 6

Solution of Differential Equations (2.36) to (2.39)

IBM 7044 Computer

Values of some of the parameters used:

$E_V^f = 0.76$ $\quad T_q = 718°K$

$\alpha = 10^{10}$ $\quad K = 8.62 \times 10^{-5}$ eV

$\nu = 10^{13}$/secs $\quad B_2 = 0.17$eV

$\lambda = 2.86$ A° $\quad E_m = 0.60$eV

$E_{m_2} = 0.50$eV $\quad I_o = 17.25 \times 10^{-4}$ atomic position

1. Annealing Temp = 273°K $\quad B_{V\text{-}Mn} = 0.10$eV

Time Seconds	V $\times 10^5$	V_2 $\times 10^7$	C $\times 10^5$	N $\times 10^5$	N/N_o
0	0.6457	0.2019 10^{-1}	0.3503 10^{-1}	0.5000	1
0.5	0.3073	0.1108	0.1904	0.4999	0.999881
30.0	0.2938	0.6427	0.1819	0.4886	0.987937
60.0	0.2865	0.6117	0.1775	0.4762	0.974919
90.0	0.2707	0.5829	0.1732	0.4646	0.962388
120.0	0.2782	0.5558	0.1692	0.4335	0.950123
150.0	0.2669	0.5305	0.1653	0.4428	0.938114
180.0	0.2608	0.5066	0.1615	0.4325	0.926353
210.0	0.2550	0.4842	0.1579	0.4226	0.908722
240.0	0.2994	0.4631	0.1545	0.4131	0.903541
270.0	0.2440	0.4432	0.1511	0.4040	0.892482
300.0	0.2388	0.4244	0.1479	0.3951	0.881637
330.0	0.2337	0.4067	0.1448	0.3867	0.871014
360.0	0.2289	0.3900	0.1418	0.3785	0.860591
390.0	0.2242	0.3741	0.1389	0.3706	0.850377
420.0	0.2196	0.3591	0.1361	0.3629	0.840353
450.0	0.2153	0.3449	0.1334	0.3555	0.830520
480.0	0.2111	0.3315	0.1308	0.3484	0.820878

2. Annealing Temp = 273°K B_{V-Mn} = 0.120eV

Time Seconds	V $\times 10^5$	V_2 $\times 10^7$	C $\times 10^5$	N $\times 10^5$	N/N_o
0	0.4646	0.2019	0.6685	0.5318	1
0.519	0.1265	0.5896	0.4041	0.5318	0.999913
30.0	0.1202	0.1070	0.4068	0.5219	0.994889
60.0	0.1195	0.1059	0.4046	0.5263	0.989541
90.0	0.1189	0.1048	0.4025	0.5235	0.984336
120.0	0.1183	0.1037	0.4004	0.5207	0.979168
150.0	0.1176	0.1026	0.3983	0.5180	0.974041
180.0	0.1170	0.1015	0.3962	0.5153	0.968956
210.0	0.1164	0.1005	0.3942	0.5126	0.963908
240.0	0.1158	0.9944	0.3921	0.5100	0.958923
270.0	0.1152	0.9841	0.3901	0.5073	0.953940
300.0	0.1146	0.9740	0.3881	0.5047	0.949012
330.0	0.1140	0.9640	0.3861	0.5021	0.944126
360.0	0.1135	0.9541	0.3841	0.4995	0.939277
390.0	0.1129	0.9444	0.3822	0.4970	0.934468
420.0	0.1123	0.9348	0.3802	0.4944	0.929693
450.0	0.1117	0.9253	0.3783	0.4919	0.924956
480.0	0.1112	0.9160	0.3764	0.4894	0.920259

Temp = 273 E_{V-Mn} = .08eV

Time Seconds	V $\times 10^5$	V_2 $\times 10^7$	C $\times 10^5$	N $\times 10^5$	N/N_o
0.0	0.4646	.2019 10^{-1}	0.3503 10^{-1}	.50002	1
0.5	0.3073	0.1108	0.1904	0.4999	.999846
30	0.2938	0.6427	0.1819	0.4886	.977091
60	0.2865	0.6117	0.1775	0.4762	.952432
90	0.2797	0.5829	0.1733	0.4646	.929196
120	0.2782	0.5559	0.1692	0.4535	.906911
150	0.2669	0.5305	0.1653	0.4428	.885519
180	0.2608	0.5066	0.1616	0.4325	.864971
210	0.2550	0.4842	0.1580	0.4226	.855204
240	0.2494	0.4631	0.1545	0.4131	.826202
270	0.2440	0.4432	0.1511	0.4040	.807909
300	0.2388	0.4244	0.1480	0.3951	.790277
330	0.2337	0.4067	0.1448	0.3867	.773292
360	0.2289	0.3900	0.1418	0.3784	.756902
390	0.2242	0.3741	0.1389	0.3706	.741097
420	0.2200	0.3591	0.1361	0.3629	.725825
450	0.2513	0.3449	0.1334	0.3555	.711071
480	0.2111	0.3315	0.1308	0.3484	.696818

Annealing Temp = 283°K $B_{V-Mn} = 0.8$

Time Seconds	V $\times 10^5$	V_2 $\times 10^7$	C $\times 10^5$	N $\times 10^5$	N/N_o
0	0.4646	0.2019	0.3503	0.5000	1
0.5	0.3198	0.2154	0.1757	0.4998	0.998826
30.0	0.3000	0.5369	0.1648	0.4755	0.90557
60.0	0.2854	0.4855	0.1568	0.4519	0.82256
90.0	0.2722	0.4419	0.1495	0.4305	0.751889
120.0	0.2599	0.4025	0.1428	0.4108	0.690113
150.0	0.2485	0.3680	0.1365	0.3924	0.635705
180.0	0.2380	0.3372	0.1307	0.3754	0.587468
210.0	0.2280	0.3096	0.1253	0.3595	0.544420
240.0	0.2187	0.2849	0.1202	0.3446	0.503850
270.0	0.2100	0.2627	0.1154	0.3307	0.471102
300.0	0.2019	0.2427	0.1109	0.3177	0.439640
330.0	0.1942	0.2246	0.1067	0.3054	0.411081
360.0	0.1870	0.2081	0.1027	0.2939	0.385028
390.0	0.1801	0.1932	0.9900	0.2830	0.361218
420.0	0.1737	0.1796	0.9546	0.2728	0.339361
450.0	0.1676	0.1672	0.9211	0.2630	0.319255
480.0	0.1618	0.1559	0.8893	0.2539	0.300725

Annealing Temp = 283°K B_{V-Mn} = 0.1eV

Time Seconds	V $\times 10^5$	V_2 $\times 10^7$	C $\times 10^5$	N $\times 10^5$	N/N_0
0	0.4646	0.2019	0.4839	0.5134	1
0.5	0.2273	0.1269	0.2834	0.5132	0.999699
30.0	0.2196	0.2868	0.2736	0.4989	0.971865
60.0	0.2133	0.2707	0.2658	0.4846	0.943925
90.0	0.2074	0.2560	0.2585	0.4711	0.917665
120.0	0.2018	0.2423	0.2515	0.4582	0.892548
150.0	0.1964	0.2295	0.2448	0.4459	0.868495
180.0	0.1913	0.2176	0.2384	0.4340	0.845444
210.0	0.1863	0.2064	0.2322	0.4227	0.823322
240.0	0.1815	0.1960	0.2263	0.4118	0.802102
270.0	0.1770	0.1862	0.2206	0.4013	0.781719
300.0	0.1726	0.1771	0.2151	0.3912	0.762113
330.0	0.1683	0.1685	0.2099	0.3816	0.743266
360.0	0.1643	0.1604	0.2048	0.3722	0.725117
390.0	0.1606	0.1529	0.1999	0.3633	0.707648
420.0	0.1565	0.1457	0.1952	0.3547	0.690802
450.0	0.1529	0.139	0.1906	0.3463	0.674556
480.0	0.1494	0.1326	0.1862	0.3383	0.658892

1 Annealing Temp = 283 °K $B_{V\text{-}Mn} = 0.12$

V $\times 10^5$	V_2 $\times 10^7$	C $\times 10^5$	N $\times 10^5$	Time Seconds	$N-N_o$
0.4646	0.2019 00^{-1}	0.6685 10^{-1}	0.5318	0.0	1
0.1385	0.7160 10^{-1}	0.3917	0.5317	0.5	.999798
0.1365	0.1108	0.3861	0.5249	30.0	.987021
0.1348	0.1079	0.3811	0.5180	60.0	.973955
0.1330	0.1051	0.3761	0.5113	90.0	.961354
0.1313	0.1024	0.3713	0.5047	120.0	.948992
0.1296	0.9985	0.3666	0.4983	150.0	.936864
0.1280	0.9733	0.3620	0.4919	180.0	.924964
0.1264	0.9490	0.3574	0.4857	210.0	.913278
0.1248	0.9253	0.3530	0.4796	240.0	.901815
0.1233	0.9024	0.3486	0.4736	270.0	.890562
0.1217	0.8802	0.3443	0.4677	300.0	.879506
0.1202	0.8587	0.3400	0.4620	330.0	.868656

Annealing Temp = 303 °K $\quad$ $B_{V-Mn} = 0.12$ eV

V $\times 10^5$	V_2 $\times 10^7$	C $\times 10^5$	N $\times 10^5$	Time Seconds	N/N_o
0.4646	0.2019×10^{-1}	0.6685×10^{-1}	0.5318	0	1
0.1737	0.1164×10^{-1}	0.3551	0.5312	0.5	0.998822
0.1737	0.1028×10^{-1}	0.3323	0.4969	30.0	0.934378
0.1520	0.8987×10^{-1}	0.3108	0.4646	60.0	0.873565
0.1425	0.7899×10^{-1}	0.2914	0.4355	90.0	0.818844
0.1338	0.6962×10^{-1}	0.2736	0.4088	120.0	0.768602
0.1258	0.6151×10^{-1}	0.2572	0.3842	150.0	0.722351
0.1184	0.5447×10^{-1}	0.2420	0.3615	180.0	0.679676
0.1115	0.4833×10^{-1}	0.2280	0.3405	210.0	0.640185
0.1051	0.4298×10^{-1}	0.2150	0.3210	240.0	0.603611
0.9923×10^{-1}	0.3829×10^{-1}	0.2030	0.3030	270.0	0.569653
0.9373×10^{-1}	0.3416×10^{-1}	0.1917	0.2861	300.0	0.538046
0.8861×10^{-1}	0.3053×10^{-1}	0.1813	0.2705	330.0	0.508619
0.8333×10^{-1}	0.2733×10^{-1}	0.1715	0.2559	360.0	0.481141
0.7987×10^{-1}	0.2450×10^{-1}	0.1624	0.2422	390.0	0.455481
0.7519×10^{-1}	0.2198×10^{-1}	0.1538	0.2295	420.0	0.431455
0.7127×10^{-1}	0.1975×10^{-1}	0.1458	0.2175	450.0	0.408946
0.6760×10^{-1}	0.1777×10^{-1}	0.1383	0.2063	480.0	0.387846

Annealing Temp = 303°K

B_{V-Mn} = 0.15 eV

Time Seconds	V $\times 10^{-6}$	V_2 $\times 10^{-8}$	C $\times 10^{-5}$	N $\times 10^{-5}$	N/N_o
0	0.4646 × 10	0.2119	0.1085	0.5735	1
0.5	0.7698	0.2566	0.4958	0.5732	0.999527
30.0	0.7532	0.2205	0.4851	0.5609	0.978010
60.0	0.7365	0.2108	0.4744	0.5485	0.956356
90.0	0.7205	0.2018	0.4641	0.5366	0.935618
120.0	0.7050	0.1932	0.4542	0.5250	0.915422
150.0	0.6898	0.1849	0.4444	0.5137	0.895747
180.0	0.6750	0.1771	0.4349	0.5027	0.876577
210.0	0.6606	0.1696	0.4256	0.4920	0.857884
240.0	0.6465	0.1625	0.4166	0.4816	0.839675
270.0	0.6329	0.1557	0.4078	0.4714	0.821927
300.0	0.6195	0.1492	0.3992	0.4615	0.804606
330.0	0.6065	0.1430	0.3908	0.4518	0.787728
360.0	0.5938	0.1370	0.3827	0.4423	0.787728
390.0	0.5814	0.1314	0.3747	0.4331	0.755197
420.0	0.5698	0.1260	0.3669	0.4241	0.739519
450.0	0.5575	0.1208	0.3594	0.4154	0.724220
480.0	0.5460	0.1159	0.3520	0.4068	0.709300

APPENDIX II

Table 8

Homogenising period for Al - 1.0 wt % Mn alloy at 500°C (Sample No. 1)

Homogenising Period Minutes	Resistivity Ω cm $\times 10^{-6}$
0	5.2994
70	5.4616
340	5.5897
580	5.6702
1240	5.7765
1772	5.8137
1952	5.8160
2040	5.8269
2160	5.8296
2220	5.8296
2400	5.8296

APPENDIX III

Table 9

Isothermal Annealing of Al - 1.0 wt % Mn alloy (Sample No. 1)
Quenching Temp = 600° ± 1°C

(i) Annealing Temp = 400°±1°C (ii) Annealing Temp = 450° ± 1°C

Annealing Time Minutes	log t	Δρ nΩcm	Annealing Time Minutes	log t	Δρ n Ωcm
120	2.0792	12.8641	60	1.7282	13.6302
480	2.6812	22.0528	180	2.2553	27.2604
1140	3.0569	34.9170	480	2.6812	40.8905
1500	3.1761	36.7548	1200	3.0792	66.7879
3300	3.5185	51.4567	1560	3.1931	70.8769
4680	3.6702	58.8076	1920	3.2833	80.0418
6720	3.8274	69.8341	3300	3.5185	109.0415
8700	3.9395	82.6983	4680	3.6702	126.7607
12600	4.1004	112.1021	6720	3.8274	155.3841
18360	4.2639	159.8833	8760	3.9425	177.1924
22680	4.3556	192.9627	12660	4.1025	203.0898
27900	4.4456	216.8533	18420	4.2653	272.6037
			22740	4.4465	365.2890
			34590	4.5387	422.5358

(iii) Annealing Temp = 500° ± 1°C			(iv) Annealing Temp = 550° ± 1°C		
Annealing Time Minutes	log t	Δρ n Ω cm	Annealing Time Minutes	log t	Δρ m Ω cm
240	2.3802	29.316	60	1.7782	16.5586
480	2.6812	40.048	240	2,3802	36.4289
720	2.8573	55.840	480	2.6812	61.2668
960	2.9823	65.612	1080	3.0334	101.0075
1200	3.0792	79.572	1500	3.1761	120.8778
1870	3.2718	106.096	1860	3.2695	135.7805
2110	3.3243	113.076	2640	3.4215	157.3067
2590	3.4133	129.828	4620	3.6646	230.1646
3250	3.5119	152.164	6660	3.8235	288.1197
3610	3.5575	161.936	8640	3.9365	326.2044
3970	3.5988	175.896	17220	4.2335	466.1246
4630	3.6656	194.044			
4990	3.6981	203.816			
5350	3.7284	212.192			
6190	3.7917	234.528			
6505	3.8132	242.764			
7165	3.855	261.331			
7585	3.8800	272.080			
7885	3.8968	279.898			
8485	3.9287	299.442			
8785	3.9437	309.214			
9445	3.9752	317.032			
10165	4.0068	338.530			
10825	4.0346	352.210			
11125	4.0464	361.005			
11545	4.0626	370.777			
12205	4.0867	391.248			
12625	4.1014	399.116			

(iii) Annealing Temp = 500° ± 1°C

Annealing Time Minutes	log t	Δρ n Ω cm
13645	4.1351	427.455
14605	4.1644	449.930
15685	4.1953	472.406
16405	4.2148	493.908
17185	4.2350	512.471
17785	4.2500	528.106
18445	4.2657	545.836
19165	4.2823	559.796
20005	4.3010	579.340
20605	4.3139	593.300
21385	4.3300	612.844
22045	4.3432	629.596
22825	4.3583	642.160
23485	4.3707	660.308
24265	4.3849	674.268
24985	4.3976	695.208
25525	4.4068	703.584
26245	4.4190	717.544
26845	4.4288	731.504
27685	4.4422	741.276
28315	4.4520	753.840
28915	4.4611	760.820
29695	4.4726	770.592
30355	4.4821	787.344
31075	4.4924	797.116
31795	4.5023	818.056
33355	4.5230	841.788
35275	4.5474	878.084

(iii) Annealing Temp = 500° ± 1°C

Annealing Time Minutes	log t	Δρ n Ω cm
36685	4.5645	903.212
38125	4.5811	928.340
39625	4.5979	949.280
40945	4.6121	968.824
43225	4.5457	1002.328
44665	4.6499	1030.248
46525	4.6676	1056.772
50545	4.7037	1102.840
55945	4.7475	1165.660
60085	4.7788	1217.312